Influence of rhamnolipid on the reductive dechlorination of tetrachloroethene by nanoscale zero-valent iron

Masterarbeit

zur Erlangung des akademischen Grades Diplomingenieur[in]

an der Universität für Bodenkultur Wien

eingereicht von

Susanne Langer, BSc

betreut von Univ. Doz. Dr. Thomas Reichenauer

Zweitbetreuerin: Ao. Univ.-Prof. Dr.nat.techn. Maria Fürhacker

AUSTRIAN INSTITUTE OF TECHNOLOGY

Universität für Bodenkultur Wien

Acknowledgments

First, I would like to thank Dr. Thomas Reichenauer for his mentoring and the plenty of time he invested in my work. I would like to thank Dr. Reichenauer and the Austrian Institute of Technology for enabling this work, which would not have been possible without the given resources and equipment.

I would also like to thank Philipp and Dorli from AIT for always helping me with my numerous questions, for their guidance and help with the experiments and the pleasant working atmosphere at AIT because of their kindness.

I would like to thank my mum for always supporting me, my brother for his encouragement and believing in me and my sister-in-law for being partners in crime. Thank you, Stephan, for your support, your patience and your interest in discussing my work with me. Thank you to my father who inspired me to love nature and for teaching me that knowledge is important. I know you would be proud of me, dad.

ABSTRACT

Tetrachloroethene (commonly known as perchloroethylene or PCE) is a severe groundwater contaminant which is difficult to remediate, hardly biodegradable and very persistent. Zero-valent iron reacts with PCE and by complete reductive dechlorination harmless end products (ethene and ethane) are formed. Nanoscale zero-valent (nZVI) iron has a high reactivity due to its high specific surface area and can be used to treat contaminated groundwater in-situ. However, the nZVI particles tend to build aggregates due to their strong magnetic attractive forces and so lose their high surface area. The aim of this work was to investigate whether the addition of the biosurfactant rhamnolipid (RL) can help hinder the aggregation of the particles which would be seen in a higher degradation rate of PCE. Lab-scale batch experiments were conducted to investigate the possible effect of RL. Five different treatment groups were compared with concentrations of RL above and below its critical micelle concentration (CMC) and three (negative) controls were done with PCE + RL, PCE + nZVI and only PCE. The samples were analysed via GC-FID and GC-TCD. The observed degradation rate constant (k_{obs}) of PCE of the samples with the lowest RL concentration (0.1 mg L^{-1}) was significantly higher than the k_{obs} of the control with only PCE + nZVI. Moreover, a significant difference was found in the degradation of PCE of the samples with the highest RL concentration (above CMC). This treatment showed significant differences from the other treatments and controls by having the highest decrease in PCE, a higher k_{obs} of PCE and a lower k_{obs} for the production of H_2. The higher degradation of PCE could not be attributed directly to a smaller particle size. There was also a shift in reaction pathway of PCE dechlorination from β-elimination to hydrogenolysis in the treatment with the highest RL concentration. Also, the production of ethene and ethane was lower and trichloroethene (TCE) accumulated.

KURZZUSAMMENFASSUNG

Tetrachlorethen (auch bekannt als Perchlorethylen oder PCE) kann das Grundwasser stark belasten und ist schwierig zu sanieren, kaum biologisch abbaubar und sehr persistent. Nullwertiges Nanoeisen (Fe0) kann zur in-situ Sanierung von kontaminierten Grundwasser angewandt werden und ist aufgrund seiner hohen spezifischen Oberfläche sehr reaktiv. Es reagiert mit PCE und durch dessen komplette reduktive Dechlorierung werden vergleichsweise harmlose Endprodukte (Ethen und Ethan) gebildet, die sehr leicht biologisch vollständig abgebaut werden können. Die nullwertigen Nanopartikel neigen jedoch stark zur Aggregation aufgrund ihrer starken magnetischen Anziehungskräfte und verlieren dadurch ihre hohe spezifische Oberfläche. Ziel dieser Arbeit war es, zu untersuchen, ob durch Zugabe von Rhamnolipid (RL) als biologisches Tensid diese Aggregatbildung verhindert werden kann, was sich durch eine höhere Abbaurate von PCE zeigen würde. Um einen möglichen Einfluss von RL zu erforschen, wurden Experimente im Labormaßstab durchgeführt. Fünf verschiedene Variationen mit Konzentrationen von RL über und unter der Kritischen Mizellbildungskonzentration (CMC von *engl.* „critical micelle concentration) und drei verschiedene (Negativ-)Kontrollen mit PCE + RL, PCE + Fe0 und nur PCE wurden verglichen. Die Proben wurden auf einer GC-FID und GC-WLD gemessen. Die beobachtete Abbaurate von PCE (k_{obs}) der Variation mit der niedrigsten RL Konzentration (0.1 mg L^{-1}) war signifikant höher als die der Kontrolle mit PCE + Fe0. Außerdem gab es signifikante Unterschiede der Variation mit der höchsten RL Konzentration (über CMC) im Vergleich zu den anderen Variationen und den Kontrollen: Sie unterschied sich signifikant durch eine größere Abnahme von PCE, eine höhere k_{obs} von PCE und eine niedrigere beobachtete Produktionsrate von H_2. Der stärkere Abbau von PCE konnte aber nicht direkt der kleineren Partikelgröße zugeordnet werden. Der Reaktionsweg von PCE verlagerte sich in den Proben mit der höchsten RL Konzentration von β-Elimination hin zu Hydrogenolyse. In diesen Proben gab es zudem eine geringere Produktion von Ethen und Ethan und eine Akkumulierung von Trichlorethen (TCE).

TABLE OF CONTENTS

Abstract

Kurzzusammenfassung

Table of contents

List of figures

List of tables

List of equations

List of abbreviations

1. Introduction 1

1.1. Tetrachloroethene 2

1.1.1. Soil and groundwater contamination with tetrachloroethene 2

1.1.2. Environmental fate and (eco)toxicity 4

1.1.3. Remediation strategies for tetrachloroethene 5

1.2. Nanoscale zero-valent iron 8

1.3. (Bio-)Surfactants 11

1.3.1. Rhamnolipid 13

1.4. Problem and aim of the work 14

2. Material and methods 16

2.1. Experimental set-up and optimization 17

2.1.1. Pre-tests regarding the interaction of PCE and surfactant and foaming 18

2.1.2. Pre-test regarding production of H_2 by different iron particles 20

2.1.3. Batch experiments with rhamnolipid 21

2.1.3. Post-test regarding loss of PCE 22

2.2. Analysis 23

2.3. Calculations 25

2.4. Statistics 29

3. Results 30

3.1. Pre-tests regarding the interaction of PCE and surfactant and foaming 30

3.2. Pre-test regarding production of H_2 by different iron particles 32

3.3. Batch experiment with rhamnolipid 33
3.4. Post-test regarding loss of PCE 45
4. Discussion 47
4.1. Pre-tests regarding the interaction of PCE and surfactant, foaming and iron particles. 47
4.2. Pre-test regarding production of H_2 by different iron particles 48
4.3. Batch experiment with rhamnolipid 49
4.3.1. Carbon mass balances 49
4.3.2. Differences of the treatment with highest RL concentration 49
4.3.3. Influence of RL on the degradation of PCE and production of H_2 50
4.3.4. Possible causes for the influence of surfactant on PCE degradation 51
4.3.5. Influence of RL on degradation products and reaction pathway 53
4.3.6. pH and ORP measurements 55
4.4. Post-test regarding loss of PCE 55
4.5. Experimental set up and method 57
4.6. Materials 59
5. Conclusion 61
References I
Appendix V

LIST OF FIGURES

Figure 1: Structural formula of tetrachloroethene 2
Figure 2: Abundance of contaminants detected on contaminated sites in a considerable amount (multiple attributions possible), x-axis is the number of occurrences. Environment Agency Austria. updated: January 2016 (Granzin & Valtl, 2016) 3
Figure 3: Conceptual model of DNAPL flow in the groundwater body (edited from NRC, 1994) 4
Figure 4: Replacement of halogen with a H-atom during hydrogenolysis 10
Figure 5: Hydrogenolysis of PCE to TCE 10
Figure 6: β-elimination of PCE and formation of DCA 10
Figure 7: Possible reaction pathways for PCE and intermediates by reacting with ZVI. Reactions 1, 3, 4, 5, 7, 9, 14, 17 and 18 are hydrogenolysis reactions (red) and reactions 2, 6, 8, and 10 proceed in the process of β-elimination reactions (blue). Reaction 11 is occurring during α-elimination (yellow) and the hydrogenation reactions (green) are 13, 15, 16 and 19 (altered from Arnolds & Roberts, 2000). 11
Figure 8: Two different structures of rhamnolipid produced by P. aeruginosa, R1 showing a mono-rhamnolipid, R2 a di-rhamnolipid (Mulligan, 2005) 13
Figure 9: Glovebox used for preparing samples with port on the right side 17
Figure 10: Overall mass of PCE (µmol) in headspace and water, corrected for headspace loss due to sampling 30
Figure 11: Aerobe pre-test with saponin to observe foaming w/o quartz sand; left side: directly after taking samples from shaker, right side: samples after 24 hours of resting; VVS 1 and VVS 3 with 0.1 g L^{-1} of saponin (>CMC), VVS 2 and VVS 4 with 0.005 g L^{-1} (<CMC); 31
Figure 12: Anaerobe pre-test with saponin and nZVI to observe foaming w/o quartz sand; left side: directly after taking samples from shaker, right side: samples after 24 hours of resting; VVS 5 and VVS 7 with 0.1 g L^{-1} of saponin (>CMC), VVS 6 and VVS 8 with 0.005 g L^{-1} (<CMC) 31
Figure 13: VVS 5 (high saponin concentration + quartz sand) after 26 hours (24 hours of shaking and 2 hours of resting), accumulated gas bubbles at bottom of foam (left side) and in pores of quartz sand (right side) 32
Figure 14: Nanofer Star, RNIP und Hög AB particles (n=3); left side: H_2 production (µmol) over time (d); right side: correlation of accum. excess pressure (mL) and H_2 production (µmol) 33
Figure 15: Amount of PCE (µmol) in the samples over time corrected for unspecific loss (n=3); deviating values of negative control with only PCE on day 5, 9 and 48 because only 2 replicates were measured on these days (of all treatment groups) 34
Figure 16: $k_{obs22,PCE}$ (h^{-1}) and c_{22}/c_0 ratio of the different treatment groups and the negative controls including standard deviation (n=3), LSD test used for grouping; different letters indicate statistical significant differences 36
Figure 17: $k_{obs22,H2}$ and amount of H_2 (µmol) at day 22 of the different treatments and the negative controls with standard deviation (n=3), LSD test used for grouping; different letters indicate statistical significant differences 37
Figure 18: Amount of TCE (µmol) in the samples until day 22 with standard deviation (n=3) 38
Figure 19: Amount of ethane and ethene (µmol) in the samples over 48 days with standard deviation (n=3) 39

Figure 20: Summation of degradation and by-products (µmol) with unidentified peaks (shown in relation to other products) and carbon mass balances for samples with 380 mg L^{-1} RL (I) and 1 mg L^{-1} RL (II)..... 41
Figure 21: pH values of different samples on day 0 (without nZVI), day 1 (after 24 hours with nZVI) and at the end of the experiment on day 48 with standard deviation (n=2) 42
Figure 22: Measured values of ORP (mV_H) for all treatments on day 0 (without nZVI), day 1 (with nZVI) and at the end of the experiment on day 48 and the ORP in the beginning (I) of the OPR measuring process and in the end (II) 43
Figure 23: PCE electron efficiency (left) and H_2 electron efficiency (right) for all treatments (n=3)..... 45
Figure 24: Loss of PCE (µmol) over time for the post-test containing PCE + H_2O and PCE + H_2O + quartz sand and the negative control with PCE from the main experiment (n=3) 46

LIST OF TABLES

Table 1: Materials used including further information and name of supplier/company..... 16
Table 2: Overview of experiments 17
Table 3: Content of samples regarding interaction of PCE and surfactant, S = saponin, SS = stock solution 19
Table 4: Content of samples regarding foaming, QS = quartz sand; S = saponin, SS = stock solution 20
Table 5: Iron particles used and their properties 20
Table 6: Overview of materials used in samples, * = RL SS + HEPES was added, all other samples contained only RL SS (without HEPES), vials 16-18 = only PCE + RL, vials 19-21 = only PCE + nZVI, vials 22-24 = only PCE; RL = rhamnolipid, SS = stock solution; 22
Table 7: Henry's solubility constant (H^{cp}) and d lnH^{cp}/d(1/T) for different substances 26
Table 8: Calculated $k_{obs22,PCE}$ (h^{-1}) for PCE of the different treatment groups including standard deviation (n=3); (*) indicates significant difference ($p<0.05$) 35
Table 9: Calculated $k_{SA22,PCE}$ (h^{-1}) of different treatment groups with standard deviation (n=3); (*) indicates significant difference ($p<0.05$) 36
Table 10: Calculated $k_{obs50\%,PCE}$ (h^{-1}) of different treatment groups with standard deviation (n=3); (*) indicates significant difference ($p<0.05$) 37
Table 11: Calculated $k_{obs22,H2}$ (µmol d^{-1}) for H_2 of the different treatment groups with standard deviation (n=3); (*) indicates significant difference ($p<0.05$) 37
Table 12: Calculated $k_{SA22,H2}$ (L µmol d^{-1} m^{-2}) for produced H_2 of different treatment groups with standard deviation (n=3); (*) indicates significant difference ($p<0.05$) 38
Table 13: Carbon mass balances (in %) for all samples on day 9, day 41 and at the end of the experiment with standard deviation (n=3); PCE values not corrected for unspecific loss 40
Table 14: Fe(0) content of samples of the different repetitions in g L^{-1} (n=3) 44
Table 15: Content of total iron in the samples of the different repetitions in g L^{-1} (n=3) 45
Table 16: k_{obs} (h^{-1}) of the two treatments of the post-test and the negative control with PCE from the main experiment..... 46
Table 17: Ratio of mg PCE in aqueous phase measured on GC-ECD to amount in aqueous phase calculated out of measured mg PCE in gaseous phase from GC-FID (n= 3), QS = quartz sand 46

LIST OF EQUATIONS

Equation 1: Oxidation of zero-valent iron and reduction of hydrogen 8
Equation 2: Oxidation of iron and reduction of oxygen and water 8
Equation 3: Hydrolysis of iron and formation of iron(II) hydroxide 9
Equation 4: Reductive dechlorination of PCE by zero-valent iron 9
Equation 5: Reduction of PCE 9
Equation 6: Henry solubility via concentration in aqueous phase and partial pressure 25
Equation 7: Van't Hoff equation for Henry's law constant 25
Equation 8: Temperature dependence of Henry's law constant 25
Equation 9: Henry solubility via concentration in gaseous phase and aqueous phase 26
Equation 10: Conversion between different Henry's law constants 26
Equation 11: Calculation of mass in aqueous phase with temperature corrected Henry's law constant 27
Equation 12: Carbon balance of the degradation reaction of PCE 27
Equation 13: Observed PCE degradation rate constant (pseudo first-order) 27
Equation 14: Observed H_2 reaction rates (zero-order) 27
Equation 15: Surface-area normalized reaction rate constant 28
Equation 16: Calculation of electrons consumed by degradation of PCE 28
Equation 17: Calculation of electron efficiency 28

LIST OF ABBREVIATIONS

AAS	atomic absorption spectroscopy
AIT	Austrian Institute of Technology
ANOVA	analysis of variance
ATSDR	Agency for Toxic Substances & Disease Registry
CHC	chlorinated hydrocarbons
CMC	critical micelle concentration
CTAB	cetyltrimethylammonium bromide
DCA	dichloroacetylene or dichloroethyne
DCE	dichloroethene or dichloroethylene (1,1-DCE, cis-DCE or trans-DCE)
DNAPL	dense non aqueous phase liquid
ECD	electron capture detector
FID	flame ionization detector
GC	gas chromatograph
GUI	graphical user interface
HEPES	2-(4-(2-hydroxyethyl)-1-piperazinyl)-ethanesulfonacid
JGR	Java Gui for R
LSD	least significant difference
MQ	millipore water
nZVI	nanoscale zero-valent iron
ORP	oxidation-reduction potential
PAH	polycyclic aromatic hydrocarbon
P&T	purge&trap
PCBs	polychlorinated biphenyls
PCE	perchloroethylene/-ethene, trivial name of tetrachloroethene
PRB	permeable reactive barrier
RL	rhamnolipid
SDS	sodium dodecyl sulfate
SS	stock solution
TCD	thermal conductivity detector
TCE	trichloroethene
VC	vinyl chloride, trivial name of chloroethene
VOC	volatile organic compound
ZVI	zero-valent iron

1. INTRODUCTION

In Europe, an estimated overall number of 2.5 million sites is potentially contaminated with a variety of more or less hazardous organic or inorganic environmental pollutants. About 340,000 of those sites (or 14%) are suspected to be contaminated and in need of remediation measures (VAN LIEDEKERKE et al., 2014). Regarding Austria, as per January 2016, there are around 2,000 sites suspected to be substantially contaminated. About 96% of the suspected heavily contaminated sites in Austria are threatening to contaminate groundwater and in the future, mineral oil and solvents are presumed to count as the major pollutants each at one third of all considerable contaminated sites (GRANZIN & VALTL, 2016).

Classical remediation methods are often very expensive, invasive and/or the contaminated site has to be treated over a long period of time. Until now, the remediation technique most commonly used for contaminated soil is to excavate and dispose it on a landfill, known as "dig and dump" or treat it in a soil treatment plant offsite. It is an invasive approach which causes high costs and becomes more difficult to perform because of increased regulatory control of landfill operations (VAN LIEDEKERKE et al., 2014). A classical approach to clean up contaminated groundwater is to install wells, extract the groundwater, treat it on the surface and pump the cleaned water back into the groundwater body or discharge it. This method is commonly known as "pump-and-treat" and leads to high maintenance and operation costs due to the often needed long treatment period (DE BOER et al., 2007; MARTENS et al., 2010). These are the two approaches most commonly used in Austria up to 2011 (VAN LIEDEKERKE et al., 2014).

Furthermore, as the sites contaminated with mineral oil and solvents are generally located in built-up areas, classical ex-situ remediation methods face restrictions (DÖRRIE & LÄNGERT-MÜHLEGGER, 2010). To select the most suitable technique for remediation, the aim of the treatment has to be clear. It is crucial to appoint whether the source or plume zone of a contamination should be remediated and whether the site has to be cleaned up or should be secured. Also, a lot of data about the site and the contamination is required to find the optimal approach.

Regarding all the disadvantages of the most commonly used treatment methods in Austria, there is a great need for in-situ, non-invasive, efficient and eco-friendly remediation approaches to better remediate soil and groundwater in the future.

1.1. Tetrachloroethene

1,1,2,2-tetrachloroethene, also called tetrachloroethylene or perchloroethylene (PCE) is a chlorinated hydrocarbon (CHC) and a colorless liquid with an ethereal odour. PCE is likely to be carcinogenic. It was first produced around 1925 in the United States and was mainly used as chemical intermediate and as solvent. It is commercially important as dry cleaning and textile-processing solvent and for cleaning metal parts in vapor degreasing operations (WEISGRAM, 2012; ATSDR, 2014).

Its chemical formula is C_2Cl_4, its chemical structure is shown in Figure 1. Tetrachloroethene has a molecular weight of 165.83 g mol^{-1}, a melting point of -22.3 °C and a boiling point of 121.3 °C. Its solubility in water at 25 °C is 206 mg L^{-1}, it has a log octanol-water partitioning coefficient (K_{OW}) of 3.40 and a log organic carbon-water partition coefficient (K_{OC}) of 2.2-2.54 (ATSDR, 2014). Chlorinated hydrocarbons also possess a low viscosity hence a good flowability and can infiltrate the soil well (WEISGRAM et al., 2012).

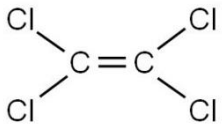

Figure 1: Structural formula of tetrachloroethene

PCE has a Henry's law constant of $1.8*10^{-2}$ atm m^3 mol^{-1} at 25 °C and a vapor pressure of 18.5 mmHg at 20 °C. Due to its high vapor pressure and Henry's law constant it is highly volatile and is classified as volatile organic compound (VOC). As its density (1.623 g mL^{-1} at 20° C) is higher than the density of water and because of its low water solubility it builds up a separate phase as a Dense-Non-Aqueous-Phase-Liquid (DNAPL) (ATSDR, 2014).

1.1.1. Soil and groundwater contamination with tetrachloroethene

In the past, as the potential hazard of tetrachloroethene was poorly understood, its use and disposal led to release into the environment through leaks and improper disposal techniques (SALE et al., 2008; SWRCB, 2014).

Tetrachloroethene is found in about half of the 1,699 hazardous waste sites proposed for inclusion on the EPA National Priorities List in the US (ATSDR, 2014). In Austria, chlorinated hydrocarbons in general are the most abundant contaminants found on contaminated sites in considerable amount (see Figure 2).

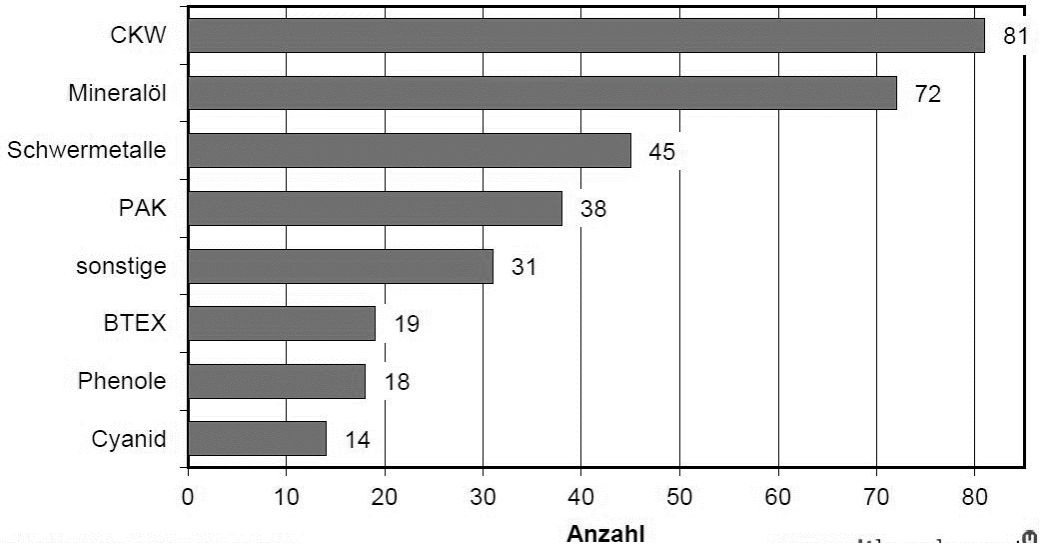

Figure 2: Abundance of contaminants detected on contaminated sites in a considerable amount (multiple attributions possible), x-axis is the number of occurrences. Environment Agency Austria. updated: January 2016 (GRANZIN & VALTL, 2016)

Regarding the exposure sources and pathways of PCE during its use nowadays, the Agency for Toxic Substances and Disease Registry (ATSDR, 2014) states for the US that release into the atmosphere plays a major role and PCE often originates from dry cleaning industry operations. Water may be contaminated by waste water released from industries like metal degreasing and soil contamination can be caused by leaking of disposal sites.

The mobility of tetrachloroethene in the soil can be seen as medium-to-high thus in surface environments its residence time is expected to be less than a few days as it evaporates into the atmosphere or leaches into the groundwater (ATSDR, 2014). If a large quantity of tetrachloroethene is spilled it moves through the soil and groundwater body due to its specific properties as separate non-aqueous, organic phase. It sinks till it reaches impermeable layers and remains there as "pool". The low interfacial tension between PCE and water allows it to easily enter pores and cracks filled with soil water. Because of its low surface tension and its viscosity, it can reach great depths in the groundwater and can also penetrate rather dense layers in the groundwater body (WEISGRAM et al., 2012). The DNAPL as separate phase follows the geological formation of an aquitard zone or of the aquiclude or bedrock material at the bottom of the groundwater body but not the direction of the groundwater flow, as shown in Figure 3. Some of the PCE phase dissolves and a plume is formed and follows the direction of the groundwater flow (see also Figure 3). A part of the contaminant also vaporizes and is found in the gaseous phase of surrounding soil pores in the vadose zone (NRC, 1994).

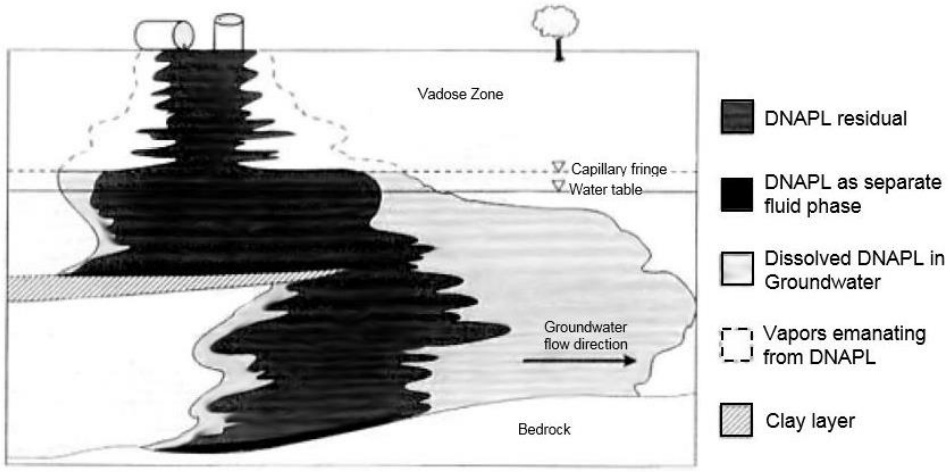

Figure 3: Conceptual model of DNAPL flow in the groundwater body (edited from NRC, 1994)

Due to its low water solubility and the formation of a separate phase tetrachloroethene is very persistent. It can reach residence times of decades in the groundwater under unfavourable circumstances and can therefore be a source of long-term contamination (LIU et al., 2005; ATSDR, 2014).

Overall, because of their characteristics, highly volatile chlorinated hydrocarbons are able to move through the soil vertically or horizontally as phase or dissolved or in their gaseous form and thereby exhibit a high mobility (GRANDEL & DAHMKE, 2008).

1.1.2. Environmental fate and (eco)toxicity

If tetrachloroethene is released in the atmosphere, long-range transport is possible and it can be found in the atmosphere worldwide. When released into surface water, PCE volatizes rapidly (ATSDR, 2014). For its fate if soil and groundwater is contaminated, see the pervious chapter 1.1.1.

It is chemically stable under aerobic conditions leading to only slow degradation in aerobic soil and groundwater (SALE et al., 2008). Natural biodegradation leads to different hazardous degradation products like the probably carcinogenic trichloroethene (TCE), possibly carcinogenic substances like 1,2-dichloroethene (cis-DCE and trans-DCE) and the carcinogenic vinyl chloride (VC) (GRANDEL & DAHMKE, 2008; WEISGRAM et al., 2012; SWRCB, 2014). Vinyl chloride and cis-DCE accumulate in the groundwater (GRANDEL & DAHMKE, 2008).

Volatile chlorinated hydrocarbons can cause narcotization, respiratory tract irritation and irritation of skin, mucous membranes and eyes. They can also lead to liver and kidney damage or damage the central nervous system (GRANDEL & DAHMKE, 2008). PCE is found to be

potentially genotoxic. It readily absorbs following inhalation (which is the main route of human exposure) or ingestion and is taken up by exposed skin. Due to its high lipophilicity it accumulates in the fatty tissue and is also found in milk. It can even distribute to the fetus by passing the placenta. If inhaled, it is adsorbed into the blood through the lungs, repeated inhalation leads to increasing concentrations in the body. There is nearly no metabolization of PCE by humans, only 1-3% is metabolized to trichloracetic acid ($C_2HCl_3O_2$) and it appears to be a saturable metabolization at high concentrations (>100 ppm). There are two different and irreversible pathways of PCE metabolization which have been found in humans, rats and mice: the first one is the oxidation by cytochrome P-450 isozymes and the second one is the glutathione conjugation Glutathione-S-transferase. If PCE is not metabolized, exhalation is the primary route of excretion. Half-lives reach up to 55 hours for adipose tissue of humans. Highest concentrations have been found in humans and animals in adipose tissue, liver and kidney regardless of the route of exposure (ATSDR, 2014).

Highly volatile CHC do not accumulate through the food chain like other CHC (e.g. PCB) (GRANDEL & DAHMKE, 2008). Although there are multiple studies addressing acute and chronic toxicity of PCE to aquatic biota of various trophic levels, there are only a few investigations showing effects of PCE on terrestrial plants and no studies concerning effects to terrestrial wildlife (HEALTH CANADA, 1993). FENT (2013) states that studies on rats have shown the LD_{50} (lethal dose with 50% mortality of test organisms) of PCE to be 2.6 g kg^{-1} and – except for TCE (4.9 g kg^{-1}) – the chlorinated degradation products show higher acute toxicity (1,1-DCE: 0.2 g kg^{-1}; VC: 0.5 g kg^{-1}; 1,2-DCE: 0.77 g kg^{-1}). The federal department HEALTH CANADA (1993) concluded in a risk assessment of PCE that it enters the environment in significant quantities but is not expected to cause adverse effects to aquatic or terrestrial biota. It only has the potential to harm terrestrial plants, especially trees. Significant groundwater and groundwater-recharged surface water contamination occurs in areas with inappropriate disposal or spills of PCE. Tetrachloroethene is therefore assessed as potential harmful to the environment.

1.1.3. Remediation strategies for tetrachloroethene

Because of the mentioned specific properties of PCE and its behaviour in the subsoil and groundwater body (chapter 1.1.1.) it is a contaminant which is not easy to remediate. Facing technical challenges makes it difficult or too expensive to clean sites contaminated with chlorinated hydrocarbons and remediation can be very costly (SALE et al., 2008). The crucial point

of any remediation approach used is its ability to access the contaminant in the subsurface (SCHRICK et al., 2004). Also, there is not one standardised best suited remediation approach for every contaminated area as the best method depends strongly on the properties of the contaminated sites (GRANDEL & DAHMKE, 2008). Remediation can be carried out *in situ* (without excavation) or *ex situ* (excavation and possible transport of contaminated material). *Ex situ* treatment can be further divided in *on site* and *off site* methods. Distinction has to be made between the decontamination of the site aiming for the removal of the pollutant and securing the contamination with the objective to stop its distribution (WEISGRAM et al., 2012). For decontamination, it is very important to remediate the source zone of a PCE contamination. This can be done by trying to mobilize the DNAPL phase by using solvents, surfactants or treat it thermally and so gradually removing the source – by pump-and-treat, air sparging or soil vapor extraction (SWRCB, 2014).

Pump-and-treat is a classical approach as mentioned in chapter 1. Installing wells and pumping the groundwater can be used to secure a site or to remediate it (WEISGRAM et al., 2012). To clean the contaminated water, after pumping the groundwater out of the ground, various treatment methods can be applied: Tetrachloroethene can be removed by passing the water through an activated carbon filtration or by using air stripping combined with filtration (NRC, 1994; WEISGRAM et al., 2012; SWRCB, 2014). Remediation of a PCE contamination by pump-and-treat is an expensive and long-lasting endeavour because, as mentioned, PCE is present in a separate phase and not readily miscible with water. If the groundwater is pumped up, only a small portion of PCE from the phase is carried along. So to flush out a modest amount of contaminant, a large amount of water is needed (NRC, 1994). The contaminant can also be present as gaseous phase in the soil or it can be sorbed to solids (SALE et al., 2008). The NATIONAL RESEARCH COUNCIL (1994) states that depending on the characteristic of the site and the contaminant, predicted times to clean up a site by pump-and-treat can range from tens to hundreds to even a thousand years on some sites. Although often applied, due to the downsides of this method other approaches are heavily investigated.

One such approach is to install a permeable reactive barrier (PRB). A PRB is used to secure a site and consists of a wall that is built perpendicular to the groundwater flow direction. The contamination plume is cleaned by passing the wall which can either consist of reactive material (e.g. reducing material such as zero-valent iron) or of adsorptive material like activated charcoal (DÖRRIE & LÄNGERT-MÜHLEGGER, 2010; MARTENS et al., 2010). PRBs are used if it is not possible to remediate the source zone of a contamination and costs are confined to

building the wall. But they also have to be installed for a long time period, the walls can get clogged and lose their permeability and the reactivity of the fill-in material is exhausted at some point (DÖRRIE & LÄNGERT-MÜHLEGGER, 2010). Deep aquifers (e.g. >30 m) can hardly be reached (WANG & ZHANG, 1997).

Another method is the in situ chemical oxidation of the contaminant using strong oxidizing agents like permanganate, peroxide or persulfate. Strong oxidants can address all chlorinated solvents but they often have to be injected multiple times, are not cost-effective for wide-spread DNAPL contamination and interact not just specifically with the contaminant. The delivery of the oxidant to the zone of contamination is the major factor for success of this method. The groundwater has to be monitored after application to preclude secondary contamination caused by the oxidant (SALE et al., 2008).

PCE can also be biodegraded through a process known as "halorespiration" where bacteria use PCE as a source of energy. The chlorinated solvent acts as electron (e^-) acceptor and H_2 as an e^- donor. PCE is reduced to TCE and further to DCE or VC, where the biological transformation may stop due to the toxicity of these substances (PIVETZ et al., 2013; SWRCB, 2014). To enhance the biological degradation, (bio)surfactant could be added to increase the bioavailability of the hydrophobic substances (SWRCB, 2014). Also, vegetable oils, lactate polymers or other substances could be injected but mixing of these substances with the contaminant in the treatment zone is most important (SALE et al., 2008). The inoculation of selected bacterial strains known to degrade the contaminant is another possibility to enhance biodegradation but they often cannot establish in the environment because of the already present indigenous microbial communities (DÖRRIE & LÄNGERT-MÜHLEGGER, 2010).

Remediation could also be done physically. These methods can be divided in thermal and pneumatic or hydraulic approaches. For thermal treatment, the heating of contaminated area (e.g. by conduction) is coupled with a soil vapour extraction to capture the vaporized chlorinated hydrocarbons. Air sparging is a pneumatic approach whereby pressured air is injected into the groundwater causing volatile contaminants like PCE to strip off along with the air into the unsaturated zone. The soil vapour also needs treatment. Physical approaches can lead to high installation costs and can have adverse effects on the soil fauna (SALE et al., 2008; DÖRRIE & LÄNGERT-MÜHLEGGER, 2010; WEISGRAM et al., 2012).

1.2. Nanoscale zero-valent iron

Zero-valent iron can be used for remediation either as (co-)precipitant to immobilize contaminants or as reducing agent. The application of zero-valent iron (ZVI) to remediate contaminated sites dates back as early as 25 years: The first field study using zero-valent iron as a permeable reactive barrier to remediate a groundwater contaminated with PCE and TCE was conducted 1991 in Canada (O'HANNESIN & GILLHAM, 1992 in GUAN et al., 2015). In this study, the zero-valent iron acted as a reducing agent and electron donor (MARTENS et al., 2010). Due to promising results, ZVI came into focus and was then extensively applied to remediate groundwater and wastewater contaminated with various contaminants (GUAN et al., 2015).

To improve the efficiency of ZVI, to overcome limitations like non-complete degradation and accumulation of undesired byproducts and to provide an alternative to the building of PRBs, nano-sized ZVI (nZVI) to dechlorinate PCBs (polychlorinated biphenyls) was first studied by WANG & ZHANG (1997) which led to further research (GUAN et al., 2015). The advantage of nZVI is its high reactivity due to its high surface area (WANG & ZHANG, 1997; LIU & LOWRY, 2006). Also, it is used in situ as the nZVI can be applied directly in the source zone of the contamination (LIU & LOWRY, 2006). Another desired effect is that it is very effective in transformation and detoxification of many contaminants (ZHANG, 2003). Dechlorination is done completely and does not stop at intermediate degradation products and only minor amounts of chlorinated intermediates are formed (WANG & ZHANG, 1997; LIU et al., 2005). The use of nZVI to remediate sites contaminated with chlorinated hydrocarbons via reductive dehalogenation can be seen as promising technique (SCHÖFTNER et al., 2015). nZVI has been applied by injecting it into the subsurface to treat chlorinated solvent plumes and DNAPL source zones (LIU & LOWRY, 2006).

Zero-valent iron is unstable in the environment and will not only react with the contaminant but also with water and oxygen in corrosion reactions. Possible reactions of Fe^0 in H_2O are given in Equations 1-3 (according to GUAN et al., 2015):

$$Fe^0 + 2\,H^+ \rightarrow Fe^{2+} + H_2\uparrow \qquad [1]$$

Equation 1: OXIDATION OF ZERO-VALENT IRON AND REDUCTION OF HYDROGEN

$$2\,Fe^0 + O_2 + 2\,H_2O \rightarrow 2\,Fe^{2+} + 4\,OH^- \qquad [2]$$

Equation 2: OXIDATION OF IRON AND REDUCTION OF OXYGEN AND WATER

$$Fe^{2+} + 2\ H_2O \rightarrow 2\ Fe(OH)_2 \downarrow + 2\ H^+ \quad [3]$$

Equation 3: HYDROLYSIS OF IRON AND FORMATION OF IRON(II) HYDROXIDE

As seen in Equation 1 and Equation 2, the oxidation of iron leads to an increase in the pH. Fe^{2+} is hydrolysed in water and iron(II) hydroxide is formed on the surface of Fe^0 (Equation 3). Fe^{2+} is not very stable and if oxygen is present it reacts rather rapidly to Fe^{3+}. Fe^{3+} is also hydrolysed and can lead to the formation of different iron(III) oxides and hydroxides like Fe_3O_4 (magnetite or iron(II, III) oxide), $Fe(OH)_3$ (bernalite or iron(III) hydroxide) or FeOOH (iron(II, III) oxide-hydroxide, e.g. goethite) depending on the availability of oxygen. The Fe^{3+} species readily precipitate (GUAN et al., 2015). Both, organic and inorganic contaminants can adsorb to the precipitating iron oxyhydroxides: the processes involved are adsorption on the aged iron oxyhydroxides and co-precipitation of contaminants by entrapment in the structure of nascent iron oxyhydroxides (NOUBACTEP, 2013).

Zero-valent iron acts as strong reducing agent and is therefore able to dechlorinate PCE according to Equation 4 (altered from ZHANG, 2003 and LIU et al., 2005):

$$4\ Fe^0 + 4\ H_2O + C_2Cl_4 \rightarrow 4\ Fe^{2+} + C_2H_4 + 4\ OH^- + 4\ Cl^- \quad [4]$$

Equation 4: REDUCTIVE DECHLORINATION OF PCE BY ZERO-VALENT IRON

The relevant half reactions of this equation are the oxidation of the nZVI and the reduction of hydrogen (see Equation 1) and the reduction of PCE itself (altered from LIU et al., 2005):

$$C_2Cl_4 + n{\bullet}e^- + n{\bullet}H^+ \rightarrow \text{products} + 4\ Cl^- \quad [5]$$

Equation 5: REDUCTION OF PCE

There are different reaction pathways leading to the dechlorination of PCE by nanoscale zero-valent iron and formation of products like ethene and ethane. In general, hydrogenolysis and β-elimination are the most important abiotic degradation mechanisms for chlorinated ethenes (GRANDEL & DAHMKE, 2008).

Hydrogenolysis is the replacement of a halogenous atom by hydrogen. It is the most common biotic catalysed reaction (GRANDEL & DAHMKE, 2008). During the hydration, the C-X bond is breaking according to Figure 4 (WOLLRAB, 2009).

Figure 4: Replacement of halogen with a H-atom during hydrogenolysis

For hydrogenolysis of one Cl-atom, one hydrogen atom and two electrons are needed and PCE is reduced to TCE (see Figure 5 altered from GRANDEL & DAHMKE, 2008).

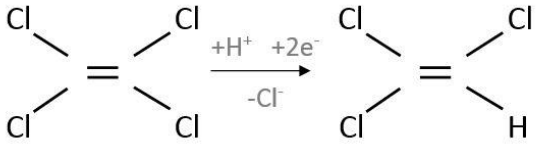

Figure 5: Hydrogenolysis of PCE to TCE

Hydrogenolysis leads to the formation of chlorinated intermediates like TCE, cis-1,2-DCE, trans-1,2-DCE, 1,1-DCE and VC (LIU et al., 2005; GRANDEL & DAHMKE, 2008). The produced cis-1,2 DCE and especially VC are both of considerable toxicological concern and are more harmful than PCE or TCE (WANG & ZHANG, 1997). Also, DCE is more water soluble and less prone to sorption than PCE hence more mobile (GRANDEL & DAHMKE, 2008).

The β-elimination (sometimes called dihaloelimination) is the release of two halogens and the formation of a triple bond as shown in Figure 6 (ROBERTS et al., 1996; GRANDEL & DAHMKE, 2008).

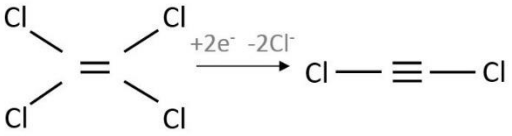

Figure 6: β-elimination of PCE and formation of DCA

In the β-elimination process, dichloroethyne or dichloroacetylene (DCA), chloroethyne and ethyne or acetylene are produced (LIU et al., 2005; GRANDEL & DAHMKE, 2008).

According to experiments conducted by ARNOLDS & ROBERTS (2000) around 87% of PCE, 97% of TCE, 94% of cis-DCE (dichlorethene) and 99% of trans-DCE are dechlorinated by reductive β-elimination. For reductive dechlorination by zero-valent iron, β-elimination is the primary pathway and hydrogenolysis is the minor pathway taken. Hence in the reaction of PCE and its degradation products with iron particles the production of more harmful intermediates like vinyl chloride is bypassed (ARNOLDS & ROBERTS, 2000; LIU et al., 2005). Figure 7 gives an overview of all possible degradation pathways and products of PCE reduction.

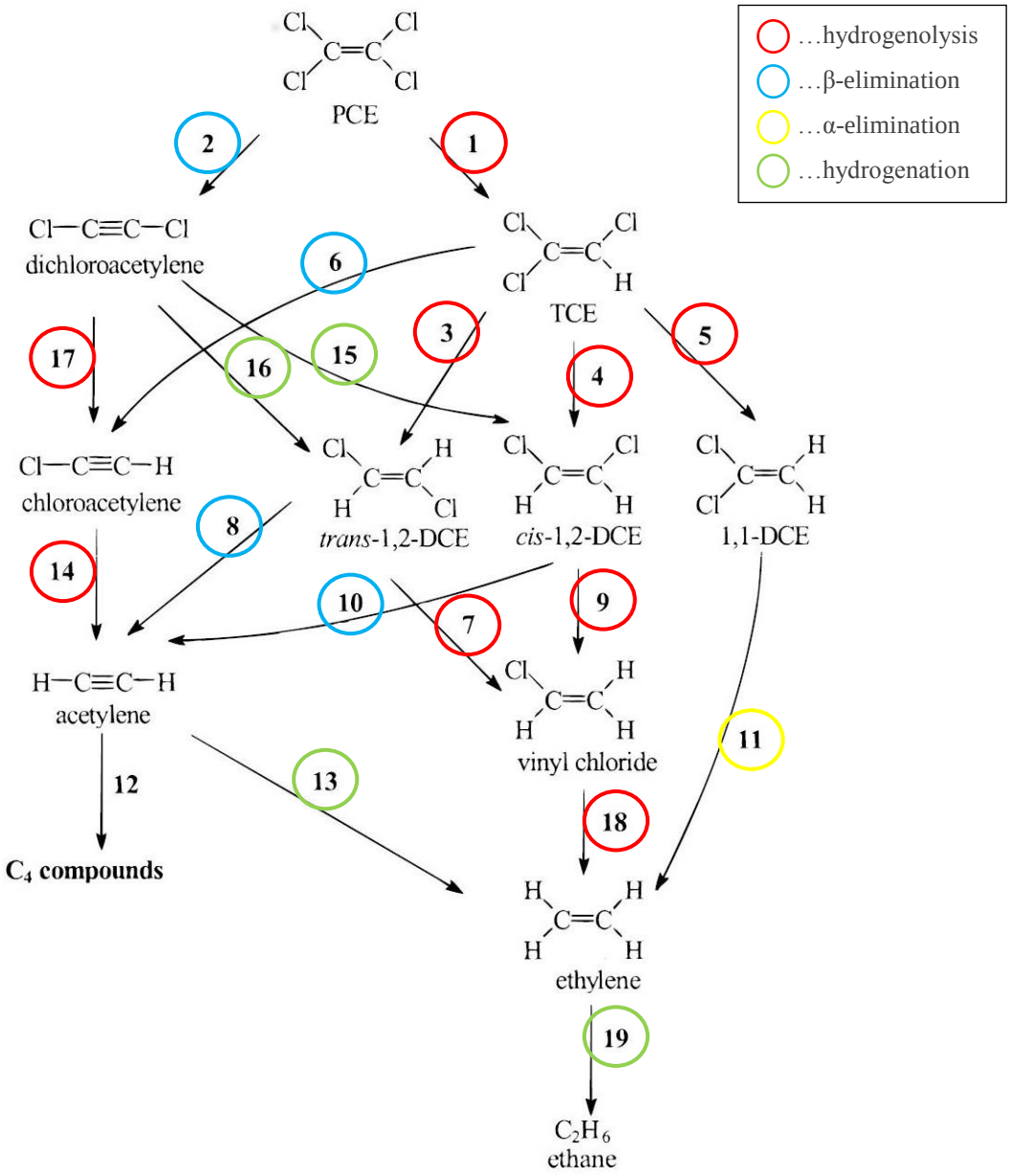

Figure 7: Possible reaction pathways for PCE and intermediates by reacting with ZVI. Reactions 1, 3, 4, 5, 7, 9, 14, 17 and 18 are hydrogenolysis reactions (red) and reactions 2, 6, 8, and 10 proceed in the process of β-elimination reactions (blue). Reaction 11 is occurring during α-elimination (yellow) and the hydrogenation reactions (green) are 13, 15, 16 and 19 (altered from ARNOLDS & ROBERTS, 2000).

1.3. (Bio-)Surfactants

Surfactants consist of a hydrophobic tail (fatty acid) and a hydrophilic head. By replacing the bulk molecules of higher energy through adsorbing on surfaces at an interface they reduce the free energy of these interfaces (ROSEN, 2004; MULLIGAN, 2005). They can lower surface tension, increase solubility, have a foaming capacity and are also known for their wetting and detergence ability. Surfactants are used as flocculating, wetting and foaming agents,

adhesives, demulsifiers and penetrants. In remediation, they can be used for soil washing or flushing as they are able to mobilize contaminants (MULLIGAN, 2005).

The most important properties of surfactants in remediation are their ability to enhance solubility, reduce surface tension and they should have a low critical micelle concentration (MULLIGAN, 2005). The critical micelle concentration (CMC) is defined as the minimum concentration at which the formation of micelles initiates meaning that further added surfactant molecules will most likely appear as micellar aggregates (RUCKENSTEIN & NAGARAJAN, 1975). This also means it is the maximum concentration of surfactant monomers in water (MULLIGAN, 2005). VOLKERING et al. (1995) studied the effect the addition of surfactant has on the biodegradation of polycyclic aromatic hydrocarbons (PAHs). They concluded that the formation of micelles by adding surfactant above the CMC lead to the micellar PAH being a reservoir. If PAH was degraded in the aqueous-phase it replenishes from these micelles. The formation of micelles therefore can interfere with the degradation of the contaminant by lowering its concentration and making the contaminant less bioavailable.

Surfactants in general can influence the bioavailability of organic compounds by dispersing non-aqueous phase liquid hydrocarbons which causes an increased contact area by reduction of interfacial tension. They can enhance the solubility of the contaminant due to the presence of micelles (containing high concentrations of contaminant) and help to transport contaminants out of the solid matrix of the soil into the aqueous phase e.g. by lowering the surface tension of pore water or by interaction of the contaminant with surfactant molecules (VOLKERING et al., 1995).

The term biosurfactants is commonly used for surfactants or surface agents of biological origin. Biosurfactants are divided in five major groups: glycolipids, phospholipids and fatty acids, lipopeptides and lipoproteins, polymeric biosurfactants and particulate biosurfactants. They can also be divided into plant and microbial produced biosurfactants whereas the second provide advantages regarding their properties and large-scale production (RANDHAWA & RAHMAN, 2014). Biosurfactants are favoured in environmental industries because of their low toxicity, their biodegradability and their effectiveness in solubilisation and enhancing biodegradation (MULLIGAN, 2005).

Biosurfactants are mostly anionic or neutral (or non-ionic), only a few are cationic e.g. those containing amine groups (MULLIGAN, 2005).

1.3.1. Rhamnolipid

Rhamnolipid (RL) is a glycolipid that is produced from *Pseudomonas aeruginosa*, *Pseudomonas sp.* and *Serratia rubidea*. Rhamnolipid is an anionic surfactant. Rhamnolipids can be divided in two types: di-rhamnolipids which consist of two rhamnose sugar molecules attached to a β-hydroxy fatty acid by the carboxyl end and mono-rhamnolipid containing only one rhamnose sugar molecule (MULLIGAN, 2005; MOHAN et al., 2006; RANDHAWA & RAHMAN, 2014). Possible chemical structures for the two different rhamnolipids are shown in Figure 8.

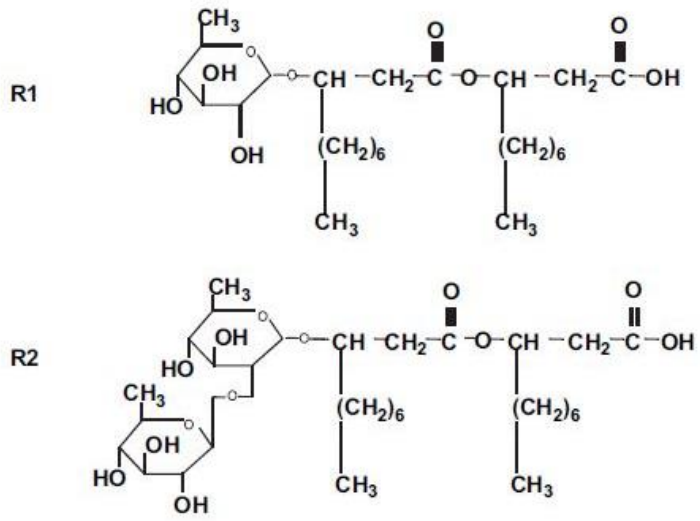

Figure 8: Two different structures of rhamnolipid produced by *P. aeruginosa*, R1 showing a mono-rhamnolipid, R2 a di-rhamnolipid (MULLIGAN, 2005)

Rhamnolipid naturally does not exist in only one type but is produced by various microorganisms as mixtures of the different types and can have diverse physicochemical properties. Four structural types can be found in rhamnolipids produced from *P. aeruginosa*: mono-rhamnolipid acid, mono-rhamnolipid methyl ester, di-rhamnolipid acid and di-rhamnolipid methyl ester. The acids possess anionic and the methyl esters non-ionic properties (ZHANG & MILLER, 1995). ZHANG & MILLER (1995) also discovered in their study that di-rhamnolipid acid and di-rhamnolipid methyl ester differ in their aqueous solubility, their produced surface and interfacial tension and their CMC. Because of that they also vary in their ability to enhance biodegradation and disperse the contaminant related to reducing the interfacial tension.

Rhamnolipids originating from *P. aeruginosa* are one of the most studied biosurfactants (MULLIGAN, 2005). MOHAN et al. (2006) have shown in respirometer tests that rhamnolipid is biodegradable in aerobic, nitrate reducing, sulphate reducing and anoxic conditions.

Two mechanisms can be the possible cause of their ability to enhance biodegradation: they may enhance the solubility of the substrate or they may interact with the cell surface and increase its hydrophobicity and therefore the ability of hydrophobic substances to associate (ZHANG & MILLER, 1995). Various studies investigating the effect of rhamnolipid on the biodegradation of organic contaminants gain different conclusions**:** NOORDMAN et al. (2002) showed in a study that RL produced from *P. aeruginosa* could enhance the biodegradation of hexadecane if the process is rate-limited. They state that rhamnolipid could help release of entrapped substances by stimulation and enhance uptake by cells. VIPULANANDAN & REN (2000) investigated the effect of rhamnolipid and of two synthetic surfactants (sodium dodecyl sulfate (SDS) and Triton X-100) on the biodegradation of naphthalene. While rhamnolipid increased the solubility of naphthalene, the degradation rate was much lower compared to that when Triton X-100 was present. They concluded that rhamnolipid was used as a carbon source instead of the contaminant and so competed with the degradation of the contaminant. ROBINSON et al. (1996) showed that the mineralization of PCB (4,4' chlorobiphenyl) was 213 times higher than that of the control if rhamnolipid (R1) was present.

Regarding the influence of rhamnolipid on contaminant degradation with nZVI, BASNET et al. (2013) conducted a study investigating the transport of Pd-doped nZVI particles stabilized with rhamnolipid (two different types), carboxy methyl cellulose and soy protein. They noticed that coated nZVI was more negatively charged. Also, the addition of surface modifiers led to a significant decrease in the extent of aggregation, with the particles coated with the two different rhamnolipids being the smallest particles.

In another study it was also concluded that rhamnolipid present during the synthesis of nZVI particles aided to maintain small sized particles. Rhamnolipid was able to disperse the particles to some amount and increased the efficiency of the conversion reaction of Cr(VI). It was concluded that rhamnolipid acts as stabilizer and provides steric hindrance by electrostatic interactions and thereby decrease aggregation. The reaction reached pseudo first order kinetics compared to second order reaction kinetics of not modified nZVI (NASSER, 2012).

1.4. Problem and aim of the work

As a major part of suspected contamination in Austria is threatening the groundwater and solvents such as tetrachloroethene are found on many of these sites, investigation is needed on the remediation of these substances. Due to the restrictions and inefficiencies of the currently most applied remediation methods there is a great need for other approaches. To use na-

noscale zero-valent iron is one such approach with the potential to remediate the source zone of a contamination in-situ, efficient, effective and in an eco-friendly way. One of the problems this method faces is that the small particles tend to aggregate due to their strong magnetic attractive forces. This effect is not desirable as with aggregation the particles become larger, lose their nanoscale size and the decrease in surface area leads to a lower reactivity of the particles. As different studies (e.g. ALESSI & LI, 2001; HARENDRA & VIPULANANDAN, 2008) have shown, the use of surfactants can help increase the degradation rate of PCE by ZVI and nZVI. Studies conducted by NASSER (2012) and BASNET et al. (2013) suggest good colloidal stability and hindering of aggregation with the use of rhamnolipid biosurfactant coated nZVI particles compared to uncoated particles.

The aim of this work was to investigate whether the addition of rhamnolipid can help hinder the aggregation of the nZVI particles so they can maintain their small size hence their high reactivity and therefore show higher PCE reduction rates than the control groups.

2. MATERIAL AND METHODS

All batch experiments were carried out using 100 mL crimp neck vials with PTFE faced stoppers and were crimped airtight with open top aluminum crimps. The main materials used for the experiments are listed in Table 1:

Table 1: Materials used including further information and name of supplier/company

device/material	**further information**	**supplier/company**
batch vials	LLG-Crimp Neck Vial ND20, 100 mL	Th. Geyer GmbH & Co. K (LGG)
stoppers	chlorobutyl-isoprene blend, PTFE faced	VWR (Wheaton)
seals	aluminum, unlined, open top	VWR (Wheaton)
purge&trap (P&T) vials	headspace screw neck vials with precision thread, ND18, 20 mL	VWR (Wheaton)
P&T caps	PP screw caps, ND18 with septum	VWR (Wheaton)
bottles	200 mL, 500 mL	Schott
100 µL syringe	100 µL gas tight glass syringe with removable needle, replaceable plunger	SGE Analytical Science
10 µL syringe	10 µL gas tight glass syringe with removable needle, replaceable plunger	Hamilton
syringe filter	<0.2 µm, non-sterile, hydrophilic, Cellulose Acetate	VWR
disposable syringe	1 mL syringe PP/PE, luer slip tip, centered, graduated, 0.01 mL	Sigma Aldrich (AGAE Techn.)
pipettes	0.1 mL, 1 mL, 5 mL, 10 mL Eppendorf Research® plus	Eppendorf
saponin	non-ionic surfactant	Sigma Aldrich
rhamnolipid	R90, 90% pure, di- and mono-RL, produced from *Pseudomonas aeruginosa*	Sigma Aldrich (AGAE Techn.)
PCE	≥ 99%, ACS grade	Sigma Aldrich
Nanofer Star	nanoscale zero-valent iron particles	NANO IRON, s.r.o. (Czech Rep.)
Höganäs AB	zero-valent iron particles in µm-scale, product name: ASC300	Höganäs Sweden AB (Sweden)
RNIP	reactive nanoscale iron particles (RNIP), product name: RNIP 10-DP	TODA KOGYO CORP (Japan)
HEPES	2-(4-[2-hydroxyethyl]-1-piperazin)-ethanesulfonic acid, pK_a = 7.48	Merck KGaA
quartz sand	natural, fire-dried; grain size: 0.5-2 mm	Min2C Natural Minerals (Austria)

2.1. Experimental set-up and optimization

Table 2 provides an overview of all different experiments carried out.

Table 2: Overview of experiments

	purpose	aqueous phase	quartz sand	PCE	surfactant	nZVI	additional information
pre-test	foaming & interaction PCE + surfactant	50 mL	-	PCE+aceton (35.56 mg L^{-1})	saponin (1-100 mg L^{-1})	-	glass beads (19 g)
pre-test	foaming with iron particles	40 mL/ 60 mL	75.75 g/ -	PCE+aceton (35.56 mg L^{-1})	saponin (5/100 mg L^{-1})	Nanofer Star (2.42 g L^{-1})	-
pre-test	formation of H_2 by diff. iron particles	40 mL	75.75 g	-	-	Nanofer Star Höganäs AB RNIP (15 g L^{-1})	-
main experiment	influence of rhamnolipid	40 mL	75.75 g	PCE (~30 mg L^{-1})	rhamnolipid (0.1-380 mg L^{-1})	Nanofer Star (2.42 g L^{-1})	8 treatments (3 replicates)
post test	loss of PCE	40 mL	75.75 g/ -	PCE (~27 mg L^{-1})	-	-	3 vials w/o sand

Millipore water (MQ) was used for preparation of all the samples and stock solutions. For anaerobic samples it was degassed using nitrogen gas (N_2) to obtain anaerobic conditions. As internal standard to ensure the tightness of the vials and to validate the calculations of headspace losses, methane (CH_4) was added to each sample in a range of 230 µL to 250 µL.

As a buffer, 2-(4-(2-hydroxyethyl)-1-piperazin)-ethanesulfonic acid (HEPES) was added in a concentration of at least 12 g L^{-1} (+0.67 g L^{-1} at a max) in all samples containing zero-valent iron to ensure pH stability at around 7.5.

All oxygen sensitive preparations were conducted in a glovebox (see Figure 9) under anoxic conditions in an argon (Ar) atmosphere. While working in the glovebox, the oxygen content

Figure 9: Glovebox used for preparing samples with port on the right side

in its atmosphere was always below 100 ppm, most of the time below 50 ppm. The materials where passed through a port which was flushed with an argon flow out of the glovebox to maintain oxygen free conditions.

The Nanofer Star particles used in all the experiments containing nanoscale zero-valent iron were stored as dry air-stable powder. Their surface is stabilized by a thin layer of iron oxides to prevent an immediate oxidation in contact with atmospheric oxygen. As the nanoparticles are clusters and agglomerates they needed to be "activated" before usage by preparation of an aqueous suspension (slurry). This was also done for the RNIP particles.

To produce this nZVI suspension, 50 g of dry Nanofer Star (or RNIP) powder was weighed in a 200 mL Schott flask in the glovebox and 200 mL of degassed MQ water were added to obtain the recommended concentration dose by the supplier (minimum amount of dry powder: 20% and maximum amount of distilled water: 80%). To disperse the nZVI and break up aggregates, the iron powder was mixed in the water using a high-shear mixer (Ultra-turrax® IKA T18, Germany) at 15,500 rpm for about 3-4 minutes. This was done in an anaerobic tent flushed with argon. The iron suspension was prepared directly before starting the experiment so it could be immediately injected into the samples with a disposable syringe (1 mL).

2.1.1. Pre-tests regarding the interaction of PCE and surfactant and foaming

Three different experiments were carried out: the first one to see if there is any degradation of PCE caused by surfactant, the second and third one to see how the foam production was influenced by the addition of quartz sand and if the samples can be shaken horizontally or have to be shaken vertically because of the formation of foam.

For the first experiment, as rhamnolipid was not yet delivered, it was reasonable to use saponin instead. The used saponin has a critical micelle concentration (CMC) of 0.1-0.01 g L^{-1} so the experiment was set up with 5 different concentrations above and below CMC (0.1 g L^{-1}, 0.05 g L^{-1}, 0.01 g L^{-1}, 0.005 g L^{-1} and 0.001 g L^{-1}) and one sample containing only PCE as negative control. The samples were prepared aerobically as no nZVI was added. PCE was used from a stock solution (SS) where it was dissolved in aceton (6 mL PCE + 35 mL aceton, concentration of PCE = 237 g L^{-1}) and 7.5 µL were added with a Hamilton gastight syringe (10 µL) to get an aqueous concentration of 35.56 mg L^{-1} in the sample vials. All vials contained 19 g of glass beads (which translates to a volume of 7 mL) to see their effect on the formation of foam. Furthermore, 250 µL of methane were added as internal standard to all vials. A saponin stock solution (1 g L^{-1}) was prepared anaerobically so it could also be used

for the foaming pre-tests by adding 0.1 g of saponin to 100 mL of degassed MQ water. The content of the samples is listed in Table 3.

Table 3: Content of samples regarding interaction of PCE and surfactant, S = saponin, SS = stock solution

name	description	saponin SS (1 g L^{-1})	MQ water	PCE SS (237 g L^{-1})
		[mL]	[mL]	[µL]
VVS 9	PCE + 0.1 g L^{-1} S	5	45	7.5
VVS 10	PCE + 0.5 g L^{-1} S	2.5	47.5	7.5
VVS 11	PCE + 0.01 g L^{-1} S	0.5	49.5	7.5
VVS 12	PCE + 0.005 g L^{-1} S	0.25	49.75	7.5
VVS 13	PCE + 0.001 g L^{-1} S	0.05	49.95	7.5
VVS 14	PCE	0	50	7.5

Overall, the samples contained 50 mL of aqueous phase, 7 mL of glass beads and 62.2 mL of gaseous phase. The samples were measured at the preparation point, vertically shaken for at least 24 hours, then taken from the shaker and left for 24 h to guarantee the collapsing of the foam before measuring the gaseous phase. This was repeated 5 more times over a duration of 39 days. The samples were measured on day 0, 2, 4, 9, 11, 15 and 39.

For the other pre-tests regarding foaming, two different sample stacks were prepared. These samples were not measured but the foam building and collapsing was observed and documented over time. The second pre-test was done aerobically and samples were done in duplicates. One set contained 75.75 g of quartz sand and 40 mL water and the other one no quartz sand and 60 mL water. The saponin stock solution was used from the first pre-test and no PCE was added to the samples. The samples were set up to have two different concentrations of saponin (0.1 g L^{-1} and 0.005 g L^{-1}) and the saponin stock solution was added to the samples like in the third pre-test shown in Table 4. They were shaken 24 hours and the stability of the foam was observed.

The third pre-test was prepared anaerobically, as nZVI was added to all the samples. The set up was identical to the second pre-test regarding the addition of quartz sand and water and the saponin stock solution. Four samples were made and the same PCE stock solution was used as in the first pre-test. It was added to the samples according to Table 4 so that the aqueous concentration was 35.56 mg L^{-1}. Also, 230 µL of methane were injected as internal standard. A suspension was made with Nanofer Star particles (as described in Chapter 2.1, p. 18) with a

concentration of 242.3 mg L^{-1}. From this suspension, 400 µL and 600 µL respectively were added to get a final concentration of 2.42 mg L^{-1} of nZVI in the samples.

Table 4: Content of samples regarding foaming, QS = quartz sand; S = saponin, SS = stock solution

name	conc. saponin [mg L^{-1}]	quartz sand [g]	saponin SS (1 g L^{-1}) [mL]	MQ water + HEPES (13.25 g L^{-1}) [mL]	PCE SS (237 g L^{-1}) [µL]	nZVI susp. (242.3 mg L^{-1}) [µL]
VVS 5	100	75.75	4	36	6	400
VVS 6	5	75.75	0.2	39.8	6	400
VVS 7	100	-	6	54	9	600
VVS 8	5	-	0.3	59.7	9	600

The samples were shaken horizontally at room temperature. It was observed if the addition of quartz sand had an influence on the foam formation and its collapsing to see which experimental set-up leads to the most favorable conditions (no or little foam or foam which collapses easily) for measuring the samples. Excess pressure caused by the production of H_2 was equalized each day.

2.1.2. Pre-test regarding production of H_2 by different iron particles

Pre-tests were conducted to see the difference in performance of three different iron particles (two particles in nanoscale and one particle in micrometer scale) by measuring the production of H_2.

The three different iron particles used are listed in Table 5 (data collected from company websites and material safety data sheets).

Table 5: Iron particles used and their properties

	particle size	composition	specific surface area (m^2 kg^{-1})
Nanofer Star	~ 50 nm	≥ 65-80 % Fe, ≤ 35-20 % FeO & Fe_3O_4	25,000
Höganäs AB	20-100 µm	98-99 % Fe	85
RNIP	~ 70 nm	70 % (50-90 %) Fe, 30 % (10-50 %) Fe_3O_4, ~1 % H_2O	28,000

For this experiment, no PCE was needed as it was carried out to observe the reaction of the iron particles with the water phase. Three replicates were done for each different iron particle. Quartz sand (75.75 g) was weighed into the sample vials and 40 mL of degassed MQ water were added. Also, 0.6 mg of Höganäs particles were weighed into the sample vials to get a concentration of 15 g L^{-1}. For the Nanofer Star and the RNIP particles, suspensions with a final concentration of 242.3 mg L^{-1} were prepared. Of these suspensions, 2.5 mL were added to the samples to obtain a final concentration of 15.14 g L^{-1}. Methane (240 µL) was injected as internal standard. The samples were measured 15 times in 98 days (on day 0, 1, 2, 6, 9, 12, 15, 19, 22, 35, 41, 48, 68, 77 and 98) and if not measured shaken at room temperature.

2.1.3. Batch experiments with rhamnolipid

To determine the effect of rhamnolipid on the reductive dechlorination of tetrachloroethene by nZVI, different treatment groups were prepared with different concentrations of rhamnolipid, a negative control with only nZVI and PCE, a negative control with only rhamnolipid and PCE and a negative control with only PCE. The rhamnolipid from Sigma Aldrich was stated to have a critical micelle concentration (CMC) of 5-380 mg L^{-1} therefore the concentrations used were 380 mg L^{-1}, 5 mg L^{-1}, 2.5 mg L^{-1}, 1 mg L^{-1} and 0.1 mg L^{-1}. For each treatment three replicates were made. As it was not possible to measure all replicates of the different treatments at the same time, the experiment was started at three time points with the same conditions and at each time point, one set of replicates of the eight different treatments was prepared. This was done to ensure that the difference caused by the new preparation of the materials was within the replicates and not within the treatment groups. The samples were measured for almost 7 weeks, precisely at day 0, 1, 2, 5, 6, 7, 9, 12, 15, 19, 22, 28, 34, 41 and 48. If not measured, the vials were covered and constantly shaken vertically at room temperature. Two times (between day 5 and 6 and between day 15 and 19), the samples were put on the shaker horizontally to thoroughly mix the test substances. Every stock solution and the nZVI suspension were prepared freshly at each time point when a new set of replicates was started.

For the batch experiments, 75.75 g of quartz sand was weighed into the 100 mL batch vials. Degassed MQ water (170 mL) was prepared in a 200 mL Schott flask and mixed with 5.5 g of HEPES to prepare the HEPES buffer. It was added to the samples according to Table 6 to ensure an overall aqueous phase volume of 40 mL (without nZVI suspension). Also, 240 µL of methane were injected as internal standard into all the samples.

The PCE stock solution was prepared in a 500 mL Schott flask with a concentration of 49 ±0.02 mg L^{-1}. This concentration is about one third of the limit of solubility of PCE and was used to ensure that the PCE was completely dissolved. For the stock solution, the Schott flask was filled to the top with degassed Millipore water (595.87 ±0.11 mL) and 18 µL of PCE (≥ 99%) were added with a syringe. It was prepared so that no headspace remained and the lid was closed tightly and wrapped with Parafilm®. The stock solution was stirred on a stirring plate for at least 24 hours to ensure the complete dissolution of the added PCE.

Rhamnolipid was used to prepare a stock solution (1 g L^{-1}) in a 200 mL Schott flask with 100 mL of degassed MQ water. To ensure that there was enough HEPES buffer in the samples with 380 mg L^{-1} rhamnolipid (as there was no MQ water with HEPES added), 90 mL of the rhamnolipid stock solution were filled in another Schott flask and were mixed with 3 g of HEPES. This solution containing rhamnolipid and HEPES was used for the sample vials 1-3 and 16-18.

Table 6: Overview of materials used in samples, * = RL SS + HEPES was added, all other samples contained only RL SS (without HEPES), vials 16-18 = only PCE + RL, vials 19-21 = only PCE + nZVI, vials 22-24 = only PCE; RL = rhamnolipid, SS = stock solution;

	conc. RL	RL SS (1 g L^{-1}) [+ HEPES* (33.3 g L^{-1})]	HEPES buffer (32 g L^{-1})	PCE SS (± 49 mg L^{-1})	nZVI susp. (242.3 mg L^{-1})	CH_4
	[mg L^{-1}]	[mL]	[mL]	[mL]	[µL]	[µL]
Vials 1-3	380	15.2*	-	24.8	400	240
Vials 4-6	5	0.2	15.0	24.8	400	240
Vials 7-9	2.5	0.1	15.1	24.8	400	240
Vials 10-12	1	0.04	15.16	24.8	400	240
Vials 13-15	0.1	0.004	15.196	24.8	400	240
Vials 16-18	380	15.2*	-	24.8	-	240
Vials 19-21	-	-	15.2	24.8	400	240
Vials 22-24	-	-	15.2	24.8	-	240

2.1.3. Post-test regarding loss of PCE

To better understand the loss of PCE in the batch experiments, a post-test was carried out. This experiment was also prepared in 100 mL vials and consisted of two samples containing quartz sand and two samples without quartz sand. No zero-valent iron or surfactant were added. The PCE stock solution (26.93 mg L^{-1}) was prepared by injecting 5 µL of PCE into a Schott flask fully filled with MQ water (301.31 mL). After stirring (with tightly closed lid and

wrapped with Parafilm®) to obtain dissolution of PCE, 40 mL of PCE Stock solution were added to all the sample vials. Methane (240 µL) was added like in the other samples and they were measured 8 times (day 0, 3, 6, 9, 13, 16, 20 and 35) for 35 days.

2.2. Analysis

Before measuring the samples, the H_2-induced excess pressure was equalized and quantified in each vial using a syringe. The concentrations of CHC and non-chlorinated hydrocarbons (HC) and of H_2 were then analyzed by taking two samples of 100 µl out of the gaseous head-space of each vial with a 100 µl gas tight syringe (SGE). These two samples were manually injected into a gas chromatograph (GC Carlo Erba, Top 8000), one sample to determine H_2 with a thermal conductivity detector (TCD) and the second sample to measure CHC and hydrocarbons via a flame ionization detector (FID). The concentrations of HC and CHC were detected with a GS-Q, 30 m, 0.53 mm plot column (Agilent J&W) and for analysis of H_2 a packed Molesieve column (5 Å) was used. Every column was equipped with its own injector block in which the sample was injected. The injector temperature was in both cases set at 110 °C. Helium (He) was used as a carrier gas (2.5 mL min^{-1}) to measure HC and CHC and argon was used as carrier gas (16 mL min^{-1}) and reference gas (17 mL min^{-1}) to measure H_2. The oven temperature program was 40 °C for 3 min, ramp 30 °C min^{-1} to 180 °C, hold for 4.8 min and then ramp 79.9 °C min^{-1} to 200 °C and hold for 5 min for best separation of the analysed species. Calibration of carbon species (methane, ethane, ethene, chloroethene) and H_2 were done using a gaseous multi-component standard and a gaseous H_2 standard (Linde AG). PCE and its degradation products (TCE, 1,1-DCE, and 1,2-cis DCE) were calibrated with liquid standards (Sigma Aldrich).

Aqueous phase concentration of tetrachloroethene was measured on a GC with an electron capture detector (ECD) for the post-tests regarding the loss of PCE. At the first 4 measuring points, the gaseous phase of the samples was measured and also a liquid sample was drawn of the aqueous phase, so the two phases were measured at the same time point. The water phase and the head space of the samples both were corrected for these losses due to the sample drawing. The gaseous phase was sampled like in the other experiments. For the liquid phase, 0.5 mL of the water phase was injected into 1 mL of hexane and stirred up briefly. These measurements on the GC-ECD were done by another research group of the same department at the Austrian Institute of Technology (AIT).

At every time point when a new repetition of the experiment was started, the Fe(0) content of the produced iron suspension was determined by injecting 100 µL of the suspension in 10 mL of degassed MQ water in a purge&trap (P&T) vial. This was done while injecting the iron suspension in the batch vials to see if the same amount of iron was injected in all the vials. The first sample for determining the Fe(0) content was made before injecting the iron suspension in the first batch vial, then the suspension was injected in three batch vials. After that, another sample was made for measuring the Fe(0) content and so on. Also in the end of injecting the iron suspension in the vials, a last sample was taken. At every start of an experiment, three to four P&T samples of the iron suspension were prepared that way. The Fe(0) content was then measured indirectly by adding 2 mL of concentrated HCl (37%) to these samples and volumetrically measuring the evolving H_2. The measured content of Fe(0) was brought in relation to the mass of iron injected into the vials. This ratio for the suspension was used as reference for the samples of the experiment.

The measurement of the Fe(0) of the samples in the beginning of the sampling process was done by gravimetrically measuring the samples before and after addition of the iron suspension. Then the mass of the added iron was multiplied with the calculated ratio of the reference samples for the iron suspension. To measure the Fe(0) content and the degree of oxidation at the end of the main experiment, the samples were shaken briefly by hand and 10 mL of supernatant were extracted using a 10 mL Eppendorf Research® plus pipette. The Fe(0) content was measured volumetrically as described above.

All these acidified samples were then stored and later used to analyse the total iron content. They were measured with an atomic absorption spectroscope (AAS, AAnalyst 400, Perkin Elmer) with a flame atomizer and a Lumina™ hollow cathode lamp for Fe.

The oxidation-reduction potential (ORP) and the pH values of the batch experiment with rhamnolipid were determined using mobile probes WTW Sentix® ORP 900 and WTW Sentix® 41. The measurement was done in the glovebox after filtration of drawn aqueous samples with a syringe filter (<0.2 µm). Replicates for these measurements for each treatment were made and treated like the samples and measured on the first day of the setup of the experiment (before adding nZVI) and on the second day of the experiment (with nZVI). All samples were opened and measured in the end of the experiment after the last sampling was done.

2.3. Calculations

To calculate the correct amounts of chlorinated and non-chlorinated hydrocarbons, hydrogen and methane, the measured values were corrected for the volumes of gas losses (pressure equalizing and drawing of the samples). CH_4 in the samples was calculated for each sampling point (also including headspace losses due to sampling and equalization of excess pressure) and these results were compared with the measured amount (see SCHÖFTNER et al., 2015).

According to SCHÖFTNER et al. (2015), the amounts of H_2, methane, propane, ethane, ethene, VC, 1,1-DCE and 1,2-cis DCE, TCE and PCE were determined in the samples. Their concentration was calculated using the Henry equation. The Henry equation states that the solubility of a gas (which is not reacting with water) is directly proportional to the partial pressure in the air space above the water phase. Henry's law constant is therefore a proportionality factor (MORTIMER & MÜLLER, 2008; SANDER, 2015). The following Equation 6-11 are all according to and with the terminology used by SANDER (2015).

The equation describing the solubility of a gas under equilibrium condition is:

$$H^{cp} = \frac{c_a}{p} \qquad [6]$$

H^{cp}… Henry solubility constant [mol m_{aq}^{-3} Pa^{-1}]
c_a… concentration in aqueous phase [mol m_{aq}^{-3}]
p… partial pressure [Pa]

Equation 6: HENRY SOLUBILITY VIA CONCENTRATION IN AQUEOUS PHASE AND PARTIAL PRESSURE

Like the change of the equilibrium constant in thermodynamics due to temperature change described in the van't Hoff equation (ATKINS & DE PAULA, 2006), the change in the Henry constant with temperature can be described as:

$$\frac{d \ln H^{cp}}{d (1/T)} = \frac{-\Delta_{sol} H}{R} \qquad [7]$$

$\Delta_{sol} H$… enthalpy of dissolution (H = enthalpy; [J mol^{-1}])
T… temperature [K]
R… ideal gas constant [8.314 J mol^{-1} K^{-1}]

Equation 7: VAN'T HOFF EQUATION FOR HENRY'S LAW CONSTANT

This equation can be used to correct the Henry constant with temperature change:

$$H(T) = H^{\ominus} \times \exp\left(\frac{-\Delta_{sol} H}{R} \left(\frac{1}{T} - \frac{1}{T^{\ominus}} \right) \right) \qquad [8]$$

$\ominus$…standard conditions

Equation 8: TEMPERATURE DEPENDENCE OF HENRY'S LAW CONSTANT

In this form, the van't Hoff equation is only valid for small changes of Δ_{sol} H and thus only for a limited temperature range. The following data (Table 7) from SANDER (1999 and 2015) were used for calculations:

Table 7: Henry's solubility constant (H^{cp}) and d lnH^{cp}/d(1/T) for different substances

substance	**H^{cp} (at T⊖)** [mol m^{-3} Pa^{-1}]	**d lnH^{cp}/d(1/T)** [K]	**Reference**
hydrogen	7.7 x 10^{-6}	500	Lide and Frederikse (1995)
methane	1.3 x 10^{-5}	1400	Reichl (1995)
ethane	2.0 x 10^{-5}	2200	Reichl (1995)
ethene	4.8 x 10^{-5}	1900	Reichl (1995)
vinyl chloride	3.7 x 10^{-4}	3300	Gossett (1987)
1,1 DCE	3.8 x 10^{-4}	3700	Gossett (1987)
1,2-cis DCE	2.6 x 10^{-3}	4200	Gossett (1987)
TCE	1.0 x 10^{-3}	4800	Gossett (1987)
PCE	5.6 x 10^{-4}	4900	Gossett (1987)
propane	1.5 x 10^{-5}	2700	Reichl (1995)

According to this data, the solubility coefficient H(T) or H^{cp} was calculated for all relevant substances. The Henry solubility coefficient can also be expressed as ratio between concentration in the aqueous phase (c_a) and the gaseous phase (c_g):

$$H^{cc} = \frac{c_a}{c_g} \quad [9]$$

H^{cc}… Henry solubility constant []
c_g… concentration in gaseous phase [mol m_g^{-3}]
c_a… concentration in aqueous phase [mol m_{aq}^{-3}]

Equation 9: HENRY SOLUBILITY VIA CONCENTRATION IN GASEOUS PHASE AND AQUEOUS PHASE

The conversion of H^{cc} to H^{cp} for an ideal gas is:

$$H^{cc} = H^{cp} \times RT \quad [10]$$

H^{cc}… Henry solubility [] via c_a and c_g
H^{cp}… Henry solubility via c_a and p
R… ideal gas constant [8.314 J mol^{-1} K^{-1}]
T… temperature [K]

Equation 10: CONVERSION BETWEEN DIFFERENT HENRY'S LAW CONSTANTS

By substituting H^{cc} in Equation 9 by Equation 10, the mass in the aqueous phase (m_a) can be calculated using the measured mass in the headspace of the vial (m_g), H^{cp} and the conversion equation:

$$m_a = \frac{m_g}{V_g} \times H^{cp} \times RT \times V_a \qquad [11]$$

V_a… volume aqueous phase [m³]
V_g… volume gaseous phase [m³]
m_a… mass in aqueous phase [g]
m_g… mass in gaseous phase [g]

Equation 11: CALCULATION OF MASS IN AQUEOUS PHASE WITH TEMPERATURE CORRECTED HENRY'S LAW CONSTANT

Using the calculated mass in the aqueous phase and in the gaseous phase, the total mass was calculated and expressed in µmol for all relevant substances. This mass was also corrected at every time point for the headspace loss of substances due to sample drawing and pressure equalization.

For every point of measurement, a carbon mass balance was calculated for each different treatment to see if the reduction in PCE fits the production of degradation products. The calculation used was Equation 12, where t_x refers to a time point in the degradation process and C (PCE_{t0}) is the amount of carbon present in PCE at the beginning of the experiment:

$$\text{C-balance} = \frac{\sum C(PCE_{tx}) + C(\text{degrad. prod.}_{tx})}{C(PCE_{t0})} \qquad [12]$$

Equation 12: CARBON BALANCE OF THE DEGRADATION REACTION OF PCE

Pseudo first-order PCE-reaction rate constants ($k_{obs,PCE}$) and zero-order H_2 reaction rates ($k_{obs,H2}$) were calculated according to Equation 13 and 14 at different time points (t_2 and t_1). The values for *c* and *n* were derived from linear regression curves (amount vs. time) for every time interval (SCHÖFTNER et al., 2015).

$$k_{obs,PCE} = -\left[\frac{\ln\left(\frac{c_2}{c_1}\right)}{t_2 - t_1}\right] \qquad [h^{-1}] \qquad [13]$$

Equation 13: OBSERVED PCE DEGRADATION RATE CONSTANT (PSEUDO FIRST-ORDER)

$$k_{obs,H2} = \left[\frac{n_2 - n_1}{t_2 - t_1}\right] \qquad [\mu mol * d^{-1}] \qquad [14]$$

Equation 14: OBSERVED H_2 REACTION RATES (ZERO-ORDER)

These reaction rates and rate constants where then normalized to the surface area of the iron particles for PCE ($k_{SA,PCE}$) [L h^{-1} m^{-2}] and for hydrogen ($k_{SA,H2}$) [L µmol d^{-1} m^{-2}]. The specific surface area of the Nanofer Star particles was assumed to be 25 m^2 g^{-1} (according to MSDS of NANO IRON, s.r.o.). Equation 15 was used to calculate these surface-area normalized rates and rate constants, with a_s representing the specific surface area of the iron particles (25 m^2 g^{-1}) and ρ_m [g L^{-1}] the total amount of iron present in the reaction vials (SCHÖFTNER et al., 2015).

$$k_{SA,PCE} \text{ or } k_{SA,H2} = \frac{k_{obs}}{a_s \times \rho_m} \quad [15]$$

Equation 15: SURFACE-AREA NORMALIZED REACTION RATE CONSTANT

According to SCHÖFTNER et al. (2015) it is important to note that not all of the contaminant is available in the aqueous phase because it is also present in the headspace where no reaction with nZVI takes place and this influences the reaction kinetics. As the PCE is degraded in the aqueous phase it is replaced by PCE dissolving from the headspace until equilibrium is installed again. The reported rate constants for degradation depend therefore on the gas/liquid ratio and are lower than the real rate constants in the water phase.

The particle efficiency is calculated to determine the efficiency of the reductive dechlorination by nZVI. It is the fraction of electrons released by oxidizing nZVI that is used to dechlorinate PCE (LIU et al., 2005). To calculate the particle efficiency, the number of electrons needed per mole of PCE dechlorination, which depends on the products formed, is used (e.g. for reduction of PCE to TCE, two electrons (n = 2) are required). The electrons for known and measured end degradation products are 8 for ethene and 10 for ethane. The electron efficiency was also calculated for H_2 (n = 2) and was done according to Equation 16 and Equation 17 (LIU et al., 2005; SCHÖFTNER et al., 2015).

$$n = \frac{\sum_i ni * pi}{\sum_i pi} \quad [16]$$

n_i… number of electrons needed for a single reaction
p_i… moles of generated end products [mol]

Equation 16: CALCULATION OF ELECTRONS CONSUMED BY DEGRADATION OF PCE

$$\epsilon = \frac{(M_0 - M_f)n}{2.5N_0} \quad [17]$$

M_0… initial amount of PCE/H_2 [mol]
M_f… final amount of PCE/H_2 [mol]
N_0… initial amount of Fe_0 added [mol]

Equation 17: CALCULATION OF ELECTRON EFFICIENCY

2.4. Statistics

Statistical analysis was performed with the statistical software *R Console* (The R Foundation, version 3.3.0, https://www.r-project.org/) and using the packages *JGR* (Java Gui for R**)** as graphical user interface (GUI) and *Deducer* as a data analysis GUI. To determine a statistical significant effect in the data, analysis of variance (ANOVA) was carried out and statistical outliers were identified using the test according to Grubbs in *Windows Excel* (Microsoft, Excel 2016). If results were statistically significant, a Tukey test and an LSD test were done for post hoc analysis. The figures were created using *SigmaPlot 12.5* (Systat Software, Inc., San Jose California, USA).

3. RESULTS

3.1. Pre-tests regarding the interaction of PCE and surfactant and foaming

The first pre-test consisting of the samples with PCE + saponin + glass beads showed no degradation of the contaminant as no degradation products were measured. Also, no excess pressure was determined. The measurements of the methane in the batches showed that the caps remained tight and headspace losses can only be attributed to sampling. Figure 10 shows a decline in PCE concentration in all samples with saponin over time.

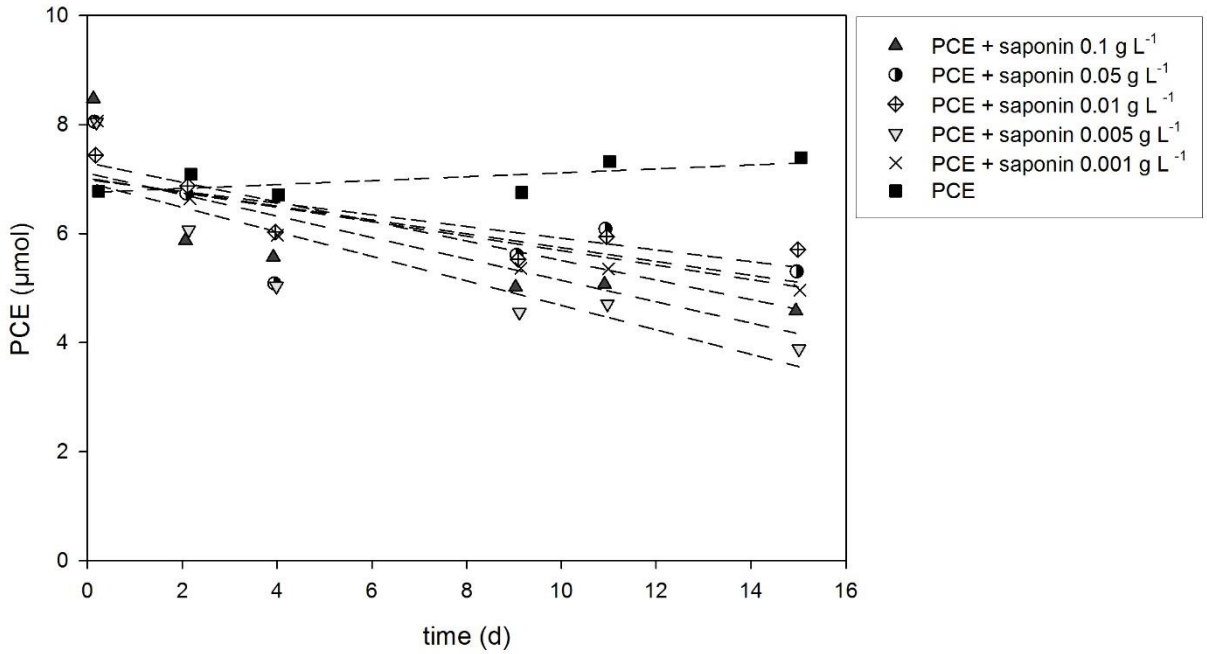

Figure 10: Overall mass of PCE (µmol) in headspace and water, corrected for headspace loss due to sampling

As there was only one repetition of each treatment group because this pre-test was done to detect a possible degradation of PCE by surfactant, no assertions can be made about standard deviations and the results only give a first insight into the interaction of PCE and surfactant.

The second pre-test was prepared to observe the stability of the developing foam caused by shaking of the vials. It was set up with or without quartz sand and with two different saponin concentrations above and below CMC (0.1 g L^{-1} and 0.005 g L^{-1}). The foam in the sample without quartz sand and with the higher saponin concentration was strongly formed and took up the whole headspace of the vial. Figure 11 shows a comparison of the samples after shaking them for 24 hours (left side) and letting them rest for 24 hours (right).

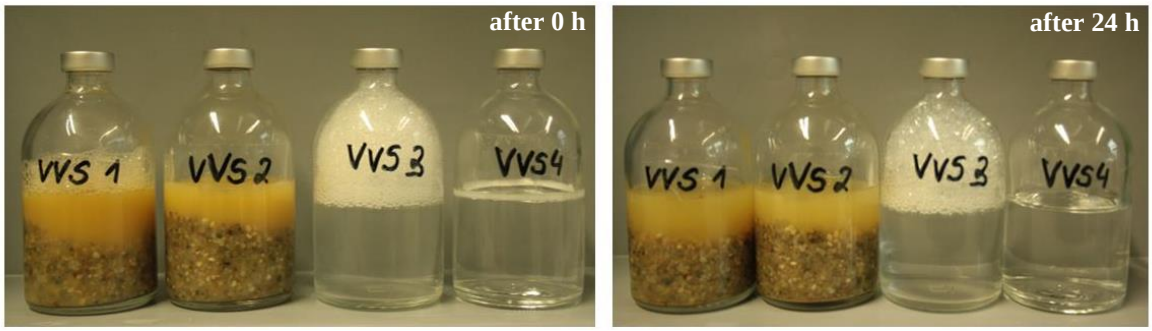

Figure 11: Aerobe pre-test with saponin to observe foaming w/o quartz sand; left side: directly after taking samples from shaker, right side: samples after 24 hours of resting; VVS 1 and VVS 3 with 0.1 g L^{-1} of saponin (>CMC), VVS 2 and VVS 4 with 0.005 g L^{-1} (<CMC);

Both samples containing high saponin concentrations (VVS 1 and VVS 3) showed a foam layer covering the complete water surface and VVS 4 with low saponin concentration and no quartz sand contained a little bit of foam. After letting the samples rest for 2 hours, the foam of VVS 1 (high saponin concentration + quartz sand) was almost completely broken down whereas there was no observable change of the foam of VVS 3. Although showing signs of breaking down (bigger bubbles), after 24 hours of resting the foam in VVS 3 still filled up almost the whole headspace (Figure 11, right side). The foam in VVS 1 was completely collapsed by then.

Figure 12: Anaerobe pre-test with saponin and nZVI to observe foaming w/o quartz sand; left side: directly after taking samples from shaker, right side: samples after 24 hours of resting; VVS 5 and VVS 7 with 0.1 g L^{-1} of saponin (>CMC), VVS 6 and VVS 8 with 0.005 g L^{-1} (<CMC)

The third pre-test with nZVI showed foaming properties similar to the second pre-test (Figure 12). The headspace of VVS 7 with high saponin concentration and no quartz sand was filled with foam after 24 hours of shaking (left side), while VVS 8 contained a little and VVS 6 no foam. The liquid phase of VVS 5 was covered with dark grey foam which took longer to break down as the foam of VVS 1 (second pre-test) containing no nZVI. After 24 hours of resting, the foam of VVS 7 still occupied half of its headspace and covered the aqueous phase completely. The foam of VVS 5 was also covering the whole water surface but the foam structure showed more signs of collapsing than the foam of VVS 7. VVS 8 contained almost

no foam. It is interesting to notice that in VVS 7 (>CMC) the nZVI is evenly distributed on the inward curved bottom of the glass vial. Compared to that, in VVS 8 (<CMC) the nZVI sunk to the walls of the vial and did not cover the whole ground of the vial (Figure 12, right side). Also, at the water-foam interface in VVS 5, outgassing H_2 and degradation products accumulated and could not pass the foam layer to reach the headspace of the vial (see Figure 13, left side). Gas bubbles were visible in the pores of the quartz sand (see Figure 13, right side).

Figure 13: VVS 5 (high saponin concentration + quartz sand) after 26 hours (24 hours of shaking and 2 hours of resting), accumulated gas bubbles at bottom of foam (left side) and in pores of quartz sand (right side)

Even after 48 hours of resting, VVS 5 and VVS 7 contained foam. The foam in VVS 5 was relatively stable, the foam in VVS 7 was more collapsed. Both covered the surface of the liquid phase. The foam in VVS 7 was almost gone on day 7 of resting. VVS 5 still contained foam, but more clinging to the walls of the vial and not covering the water phase.

3.2. Pre-test regarding production of H_2 by different iron particles

This pre-test showed that nanoscale particles (Nanofer Star and RNIP) produced more H_2 overall and in a shorter time span than the micrometer particles (Hög AB). The measured H_2 fits the measured excess pressure of the samples (Figure 14, right side). The observed zero-order reaction rate constant (k_{obs}) of H_2 for the Nanofer Star particles was highest with 4.91 ±0.28 µmol d^{-1}, followed by RNIP particles with 2.83 ±0.61 µmol d^{-1} and Hög AB particles with 0.49 ±0.15 µmol d^{-1}. These observed reaction rates of H_2 differ significantly between the different particles ($p<0.001$). If brought in relation to the surface area of the iron particles (k_{SA}), Hög AB particles had the highest k_{SA} with 0.383 ±0.099 L µmol d^{-1} m^{-2}. Nanofer Star (0.013 ±0.001 L µmol d^{-1} m^{-2}) and RNIP particles (0.006 ±0.001 L µmol d^{-1} m^{-2}) did not reach such high reaction rates. As the samples were not weighed in the beginning to

gravimetrically determine the iron content, the k_{SA} was determined using the theoretical calculated iron content in the samples. The difference in k_{SA} of the particles was also significant (*p=0.003*).

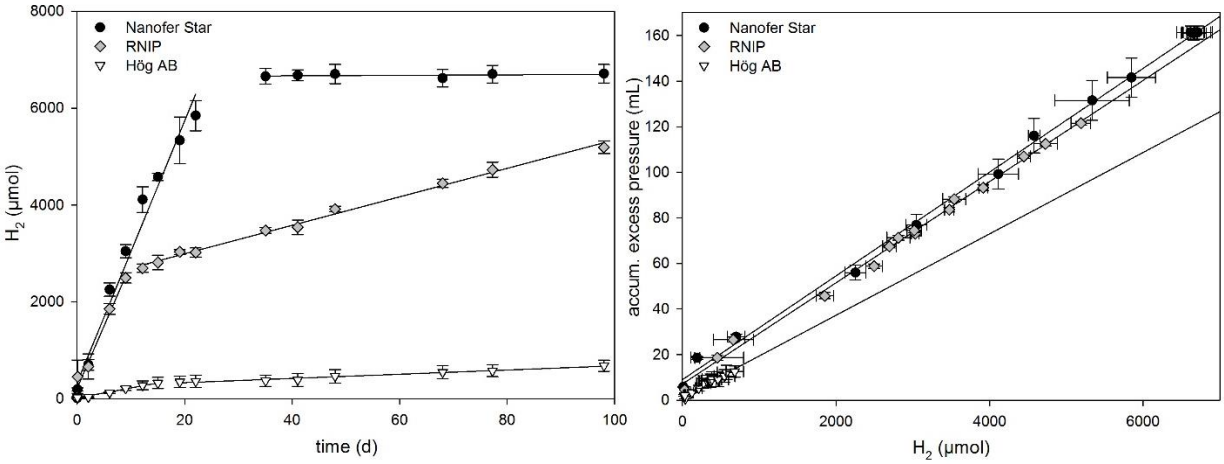

Figure 14: Nanofer Star, RNIP und Hög AB particles (*n=3*); left side: H_2 production (µmol) over time (d); right side: correlation of accum. excess pressure (mL) and H_2 production (µmol)

The production of H_2 of the Nanofer Star particles peaked somewhere between the measurement points of day 22 and day 35. After that, no new hydrogen was produced (Figure 14, left side). About 60% of the overall amount of H_2 of the RNIP particles was produced in the first 19 days resulting in production of the other 40% in the remaining 79 days. Furthermore, half of the H_2 built from Hög AB particles was produced in the first 22 days. Although production of H_2 in the samples with Nanofer Star particles stopped between day 22 and 35, the amount of H_2 in samples with RNIP und Hög AB was still increasing even in the period between the last two measurement points (day 77 and day 98).

3.3. Batch experiment with rhamnolipid

In all samples of the batch experiment with rhamnolipid, the amount of PCE measured in the headspace decreased – albeit corrected for headspace loss due to sampling and the release of excess pressure – even in the negative control samples containing only PCE. To exclude this unspecific loss in PCE, the measured values of every treatment group were corrected for the decline in PCE in the negative control samples with only PCE. For this, the absolute loss in PCE in the negative control group with only PCE was brought in relation to the mass it should contain. The measured values of PCE in the other treatments were multiplied with this ratio. The corrected values for PCE are shown in Figure 15.

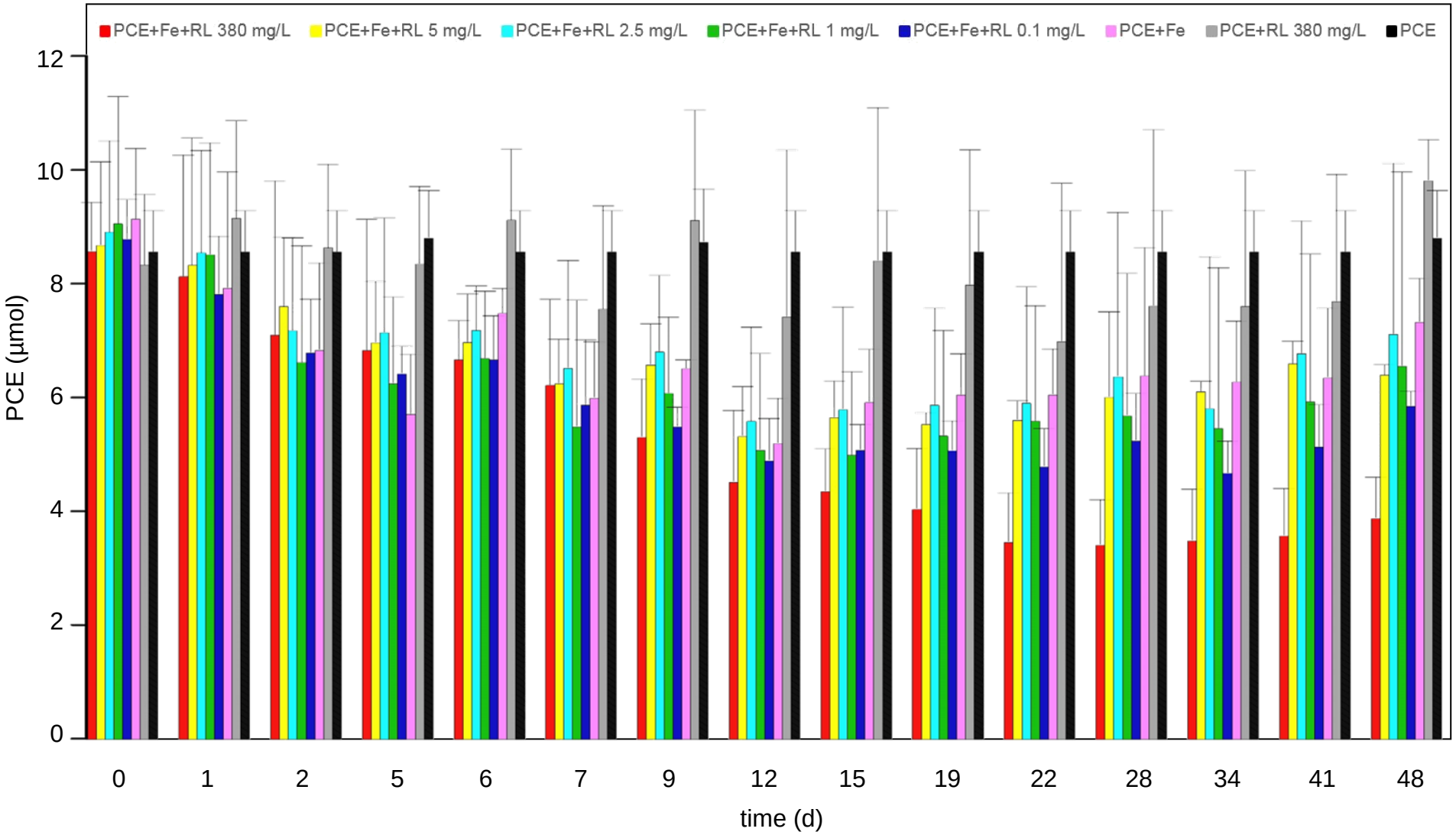

Figure 15: Amount of PCE (µmol) in the samples over time corrected for unspecific loss (*n=3);* deviating values of negative control with only PCE on day 5, 9 and 48 because only 2 replicates were measured on these days (of all treatment groups)

It is evident regarding the standard deviations of the samples containing nZVI, PCE and different concentrations of RL, that there is no clear difference in the reduction of PCE. The treatment group with 380 mg L^{-1} shows the greatest and statistically significant ($p<0.05$) decrease in PCE (red column in Figure 15). The treatment group with the second highest decline is the group containing the lowest concentration of rhamnolipid (0.1 mg L^{-1}) which does not differ significantly from the other treatments. All the other treatment groups with different RL concentrations and the samples with only PCE + nZVI show an almost similar reduction of PCE. The negative control group with PCE + RL is relatively constant over time.

At day 22, most of the samples reached their lowest PCE concentration of the experiment time of 48 days. After that, the PCE concentration did not decrease further or – if corrected for the unspecific loss – slightly increased in some samples due to the correction calculations but not because of an increase in PCE. The first-order reaction rate constants for the different treatment groups (k_{obs}) were therefore calculated for the first 22 days of the experiment and are displayed in Table 8.

Table 8: Calculated $k_{obs22,PCE}$ (h^{-1}) for PCE of the different treatment groups including standard deviation ($n=3$); $^{(*)}$ indicates significant difference ($p<0.05$)

	380 mg L^{-1}	**5 mg L^{-1}**	**2.5 mg L^{-1}**	**1 mg L^{-1}**	**0.1 mg L^{-1}**	**PCE + nZVI**	**PCE + RL**	**PCE**
$k_{obs22,PCE}$	16.19E-04$^{(*)}$	8.35E-04	8.00E-04	8.63E-04	9.92E-04$^{(*)}$	5.17E-04	5.57E-04	0$^{(*)}$
std. dev.	1.25E-04	2.89E-04	2.74E-04	3.11E-04	2.01E-04	1.69E-04	3.36E-04	0
s.d. in %	7.7	34.7	34.2	36.1	20.3	32.6	60.4	0

The $k_{obs22,PCE}$ for the different treatments showed a significant difference ($p<0.001$). Obviously, the negative control containing only PCE (which was corrected to have no loss and therefore has a $k_{obs22,PCE}$ of 0) significantly differs from all other treatments. The post hoc Tukey test also revealed that the $k_{obs22,PCE}$ of the samples containing 380 mg L^{-1} RL differed significantly ($p<0.05$) from all other treatments containing PCE, RL and nZVI and the negative control group containing only PCE + RL. Furthermore, the treatment group with a RL concentration of 0.1 mg L^{-1} differed significantly ($p<0.05$) from the negative controls with PCE + RL and PCE + nZVI. There were no significant differences between all other treatment groups.

Figure 16 shows the $k_{obs22,PCE}$ of the different treatments and in comparison, the ratio of concentration at day 22 (c_{22}) and their initial concentration (c_0) to see the differences not only in the observed reaction rate constants but also in the reduction of the PCE concentration. The LSD test used to group the $k_{obs22,PCE}$ of the different treatments underlined the results of the ANOVA.

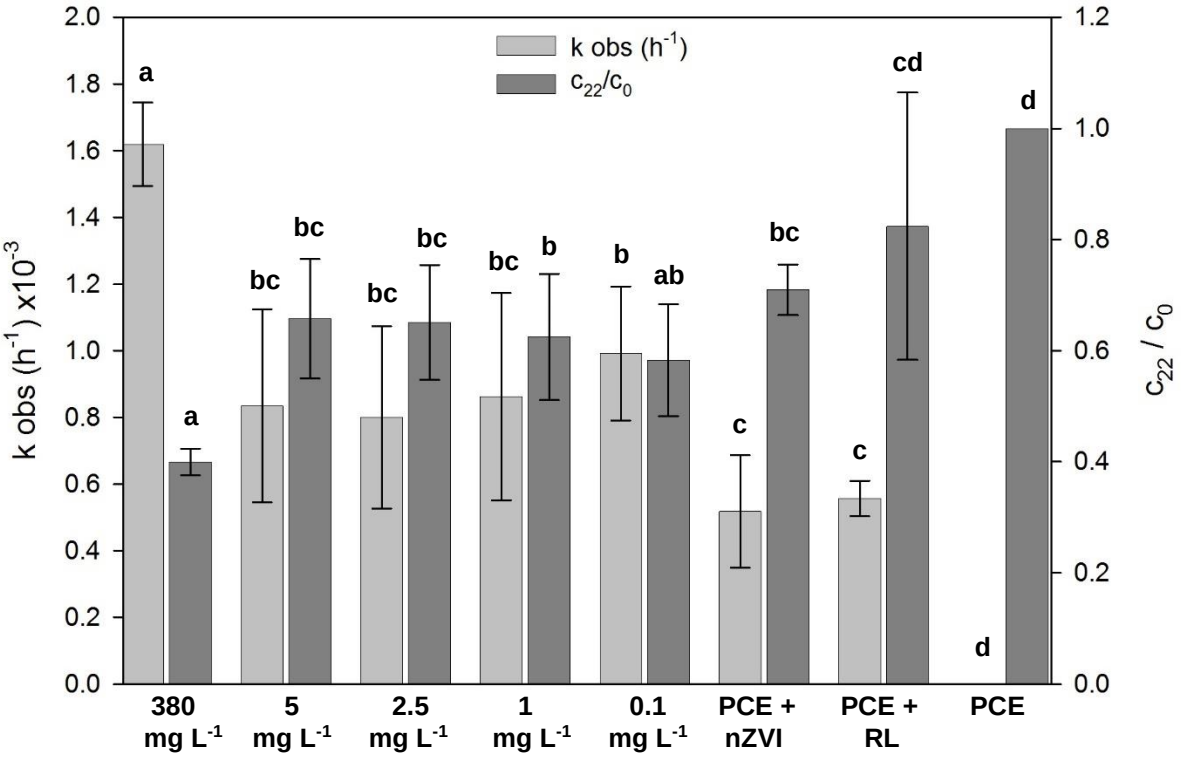

Figure 16: $k_{obs22,PCE}$ (h^{-1}) and c_{22}/c_0 ratio of the different treatment groups and the negative controls including standard deviation (*n=3*), LSD test used for grouping; different letters indicate statistical significant differences

The $k_{SA22,PCE}$ was determined using the specific surface area of the Nanofer Star particles and the total iron content (Table 9). The treatment group containing 380 mg L^{-1} RL differed statistically form the other groups ($p<0.05$). According to the Tukey test, also the treatment group with 0.1 mg L^{-1} RL differed significantly ($p=0.03$) from the negative control with PCE + nZVI. The LSD test did not show this difference as significant.

Table 9: Calculated $k_{SA22,PCE}$ (h^{-1}) of different treatment groups with standard deviation (*n=3*); (*) indicates significant difference ($p<0.05$)

	380 mg L^{-1}	**5 mg L^{-1}**	**2.5 mg L^{-1}**	**1 mg L^{-1}**	**0.1 mg L^{-1}**	**PCE + nZVI**
$k_{SA22,PCE}$	2.80e-05(*)	1.45e-05	1.40e-05	1.54e-05	1.72e-05	0.91e-05
std. dev.	0.16e-05	0.38e-05	0.36e-05	0.46e-05	0.29e-05	0.24e-05
s.d. in %	5.7	26.2	26.0	30.2	16.8	25.9

The first-order reaction rate was also calculated for the period until half of the initial PCE concentration was reached ($k_{obs50\%,PCE}$). If the amount of PCE was never this low, it was calculated for the time point with the lowest concentration reached during the experiment. Most of the samples (75%) reached half of the PCE concentration or their lowest PCE concentration in the first 12 to 15 days. The $k_{obs50\%,PCE}$ are shown in Table 10. The only group signifi-

cantly different than the other experimental groups is the negative control containing PCE ($p<0.05$). All other treatments show no significant difference in the calculated $k_{obs50\%,PCE}$.

Table 10: Calculated $k_{obs50\%,PCE}$ (h^{-1}) of different treatment groups with standard deviation ($n=3$); $^{(*)}$ indicates significant difference ($p<0.05$)

	380 mg L^{-1}	5 mg L^{-1}	2.5 mg L^{-1}	1 mg L^{-1}	0.1 mg L^{-1}	PCE + nZVI	PCE + RL	PCE
$k_{obs50\%,PCE}$	20.50E-04	13.03E-04	15.22E-04	13.54E-04	13.31E-04	14.47E-04	14.83E-04	$0^{(*)}$
std. dev.	2.33E-04	3.23E-04	2.65E-04	1.67E-04	3.95E-04	6.27E-04	15.76E-04	0
s.d. in %	11.4	24.8	17.4	12.3	29.7	43.3	106.2	0

Furthermore, the zero-order reaction rate constant of the production of H_2 ($k_{obs,H2}$) in all the samples was calculated for the first 22 days of the experiment (Table 11).

Table 11: Calculated $k_{obs22,H2}$ (µmol d^{-1}) for H_2 of the different treatment groups with standard deviation ($n=3$); $^{(*)}$ indicates significant difference ($p<0.05$)

	380 mg L^{-1}	5 mg L^{-1}	2.5 mg L^{-1}	1 mg L^{-1}	0.1 mg L^{-1}	PCE + nZVI	PCE + RL	PCE
$k_{obs22,H2}$	$105.1^{(*)}$	165.8	154.1	150.0	149.8	173.0	$0^{(*)}$	$0^{(*)}$
std. dev.	15.3	13.0	30.6	32.0	29.7	8.8	0	0
s.d. in %	14.5	7.9	19.9	21.3	19.8	5.1	0	0

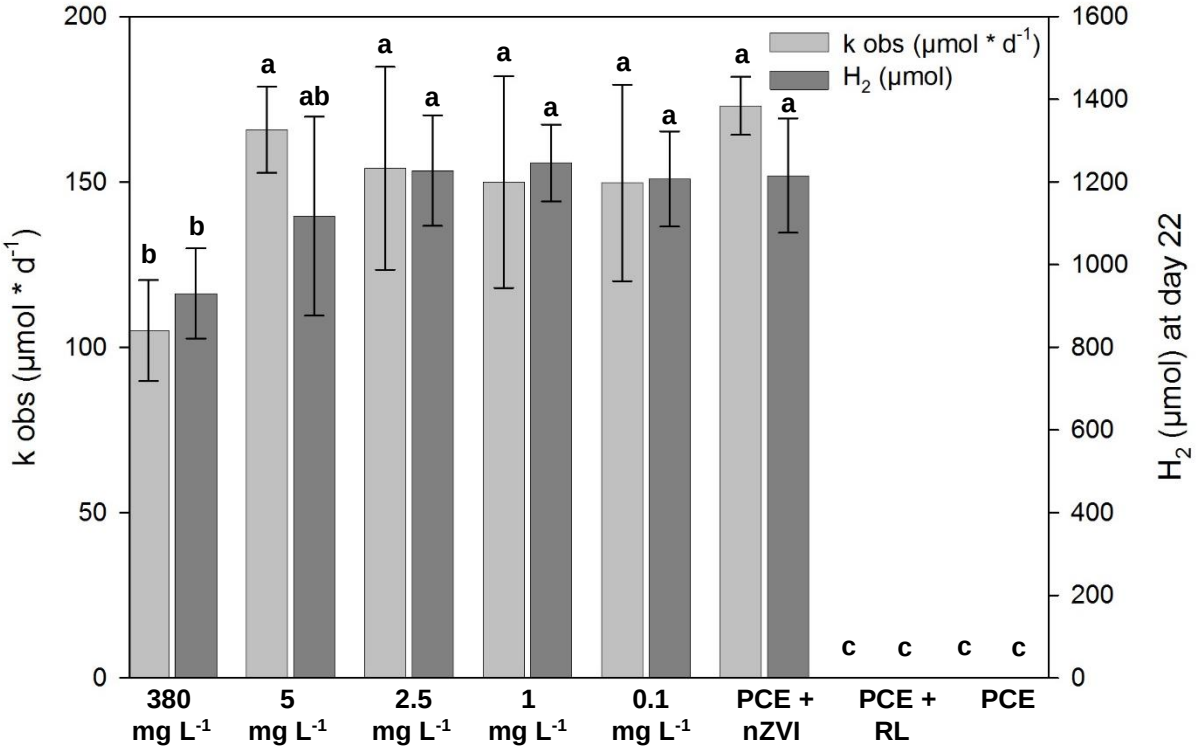

Figure 17: $k_{obs22,H2}$ and amount of H_2 (µmol) at day 22 of the different treatments and the negative controls with standard deviation ($n=3$), LSD test used for grouping; different letters indicate statistical significant differences

The calculated $k_{obs22,H2}$ for H_2 differed significantly (*p<0.001)* between the different sample groups. The Tukey test revealed a significant difference (*p<0.05*) of all groups compared to the negative controls containing PCE + RL and only PCE. Also, the $k_{obs22,H2}$ of the treatment group with a RL concentration of 380 mg L^{-1} was significantly lower (*p<0.05*) than all the other treatments. The LSD test underlined these results and marked the same treatments as significantly different (see Figure 17).

For H_2, also the $k_{SA22,H2}$ was calculated (Table 12). There was also a significant difference (*p<0.05*) like for the $k_{obs22,H2}$ between the treatment with 380 mg L^{-1} RL and the other treatment groups.

Table 12: Calculated $k_{SA22,H2}$ (L µmol d^{-1} m^{-2}) for produced H_2 of different treatment groups with standard deviation (*n=3*); (*) indicates significant difference (*p<0.05*)

	380 mg L^{-1}	**5 mg L^{-1}**	**2.5 mg L^{-1}**	**1 mg L^{-1}**	**0.1 mg L^{-1}**	**PCE + nZVI**
$k_{SA,H2}$	1.817(*)	2.894	2.712	2.670	2.591	3.058
std. dev.	0.204	0.236	0.331	0.471	0.412	0.150
s.d. in %	11.2	8.2	12.2	17.6	15.9	4.9

To see if the PCE in the samples was reduced by degradation, different degradation products and by-products of the reaction were determined.

The production of TCE is shown in Figure 18.

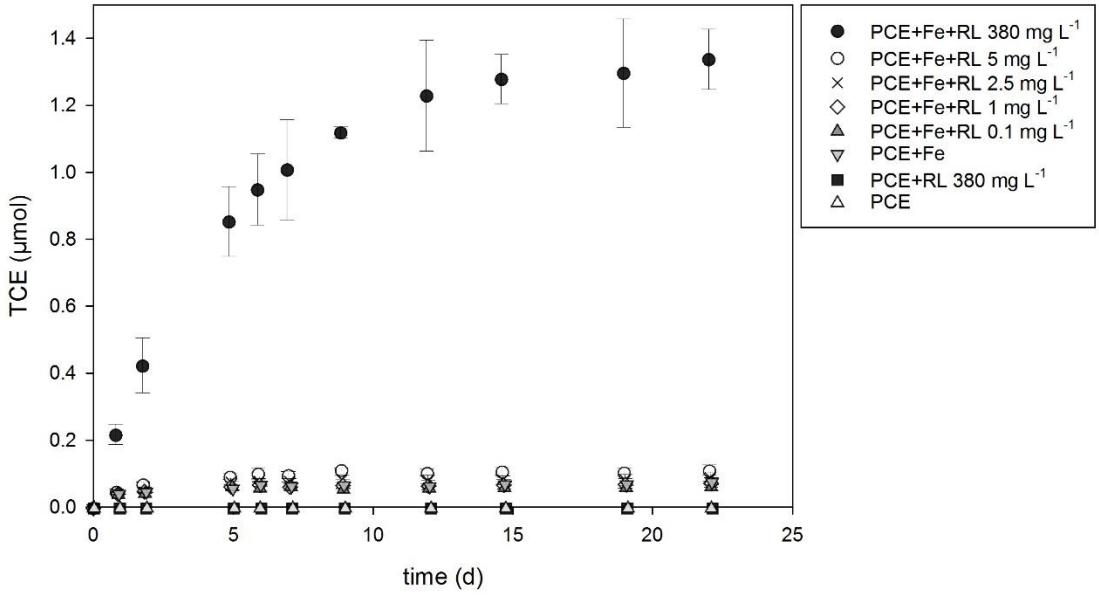

Figure 18: Amount of TCE (µmol) in the samples until day 22 with standard deviation (*n=3*)

The production of TCE also peaked at around day 22 of the experiment. The treatment with 380 mg L^{-1} RL showed the highest production of TCE with around 1.34 µmol at day 22. The ANOVA for TCE on day 22 showed a significant difference ($p<0.001$) of the samples with 380 mg L^{-1} RL compared to all the other treatments. Further, because there was no TCE in the negative controls with PCE + RL and only PCE, they also differed significantly ($p<0.05$).

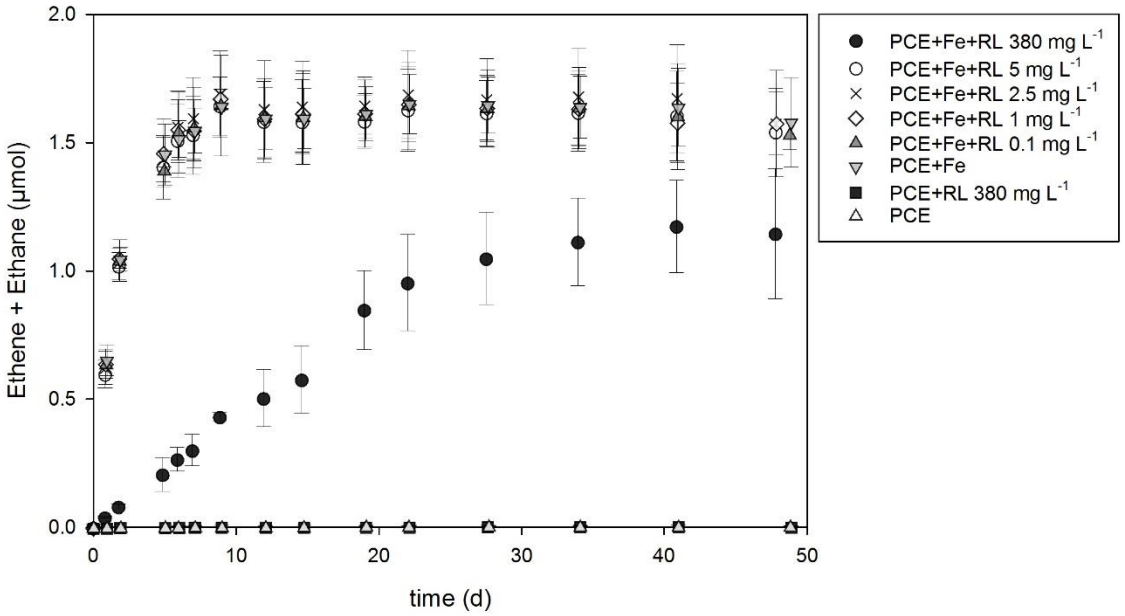

Figure 19: Amount of ethane and ethene (µmol) in the samples over 48 days with standard deviation ($n=3$)

The production of ethane and ethene is shown in Figure 19. In the negative controls with only PCE and PCE + RL, no ethane and ethene were produced. The amount of ethane and ethene in the samples with a concentration of 380 mg L^{-1} RL reached its highest value at day 41. In the other treatments with different concentrations of RL and in the control with PCE + nZVI, the production of ethane and ethene was identical and peaked at around day 9. The statistical analysis of the amounts of ethane and ethene on day 12 shows the same results as the analysis of TCE: The negative controls with PCE and PCE + RL differ significantly ($p<0.001$) because no ethane and ethene were built. The treatment with 380 mg L^{-1} RL ($p<0.05$) differs from all the other treatment groups. The ANOVA for the amounts of ethane and ethene on day 41 shows the same result ($p<0.001$). The ratio of ethene to ethane was about 61 % to 39 % in all the samples in the end. At the start of the experiment, there were about 65 % of ethene and 35 % of ethane. The exception was the treatment with the highest RL concentration: the ratio was about 61 % ethene and 39 % ethane in the beginning and 57 % to 43 % in the end.

Other degradation and by-products measured were VC, 1,1-DCE, cis-DCE and propane. They were present in small concentrations except in the negative controls with only PCE and PCE + RL. In the control samples containing only PCE + nZVI, vinyl chloride was measurable in a small amount (0.016 ±0.006 µmol) and in all the other treatments it was below the limit of quantification. In the samples containing 380 mg L^{-1} RL, 1,1 DCE was quantifiable, contrarily to all other treatments. The first detectable measured amount on day 6 was 0.021 ±0.006 µmol. It increased steadily over time till reaching 0.056 ±0.011 µmol at the end of the experiment. Cis-DCE, like 1,1 DCE, was measured with 0.023 ±0.020 µmol on day 5 and 0.139 ±0.098 µmol on day 48 in the samples with 380 mg L^{-1} RL. There was also a continuous linear increase in cis-DCE. Further, propane was detected on day 15 in the treatment with 380 mg L^{-1} RL with an amount of 0.010 ±0.002 µmol. The amount of propane as well increased linearly to 0.032 ±0.004 µmol on day 48. For all the other treatments containing nZVI, propane was first detected on day 6 with an amount of 0.013 ±0.001 µmol. This amount remained constant in all these samples until the end of the experiment.

The carbon mass balance shows if the production of degradation products and by-products corresponds with the reduction in PCE. It was calculated for all the samples without correction for the unspecific loss of PCE. The carbon mass balance showed an exponential decline for all treatments until reaching about 55 ±4 % at day 48 (see Table 13).

Table 13: Carbon mass balances (in %) for all samples on day 9, day 41 and at the end of the experiment with standard deviation (*n=3*); PCE values not corrected for unspecific loss

	380 mg L^{-1}	**5 mg L^{-1}**	**2.5 mg L^{-1}**	**1 mg L^{-1}**	**0.1 mg L^{-1}**	**PCE + nZVI**	**PCE + RL**	**PCE**
day 9	**65.9** ±0.5	**75.9** ±13.9	**73.1** ±6.7	**71.0** ±9.4	**67.1** ±10.3	**73.5** ±11.7	**82.3** ±1.0	**72.5** ±0.6
day 41	**55.6** ±6.5	**63.9** ±16.8	**60.6** ±4.7	**54.3** ±3.0	**55.4** ±13.5	**61.1** ±7.8	**49.8** ±5.2	**53.6** ±9.1
day 48	**52.9** ±4.0	**58.6** ±14.0	**58.0** ±6.3	**52.1** ±5.5	**54.2** ±5.4	**62.4** ±12.4	**51.3** ±13.1	**50.0** ±8.6

The treatment with PCE + nZVI showed the highest carbon mass balance with a value of 62.4 % and the negative control with only PCE having the greatest decline and reaching only 50 % in the end of the experiment. Figure 20 depicts the carbon mass balances for two different treatments, 380 mg L^{-1} RL and 1 mg L^{-1} RL. The treatment with 1 mg L^{-1} RL was used as an example of all the samples containing RL + nZVI because they looked similar. Figure 20 shows the content of PCE and the degradation and by-products of the reductive dechlorination process. It also includes the unidentifiable peaks found in every sample which could not be qualified but were set in relation to the other products. As it is shown in Figure 20 (II) for the

treatment with 1 mg L^{-1} RL, almost no TCE and other degradation products were built. Ethane and ethene were produced in the first days of the experiment and then the amount remained constant. The same trend can be observed for the unidentified other substances. In contrast, in the samples containing 380 mg L^{-1} (Figure 20, I), less ethane and ethene were built and at a slower rate. Further, the unidentified substances increased at a slower rate and more TCE, 1,1-DCE, cis-DCE and propane were produced than in the other treatments with RL and nZVI. The carbon mass balances in both treatments decreased by almost half, as mentioned before.

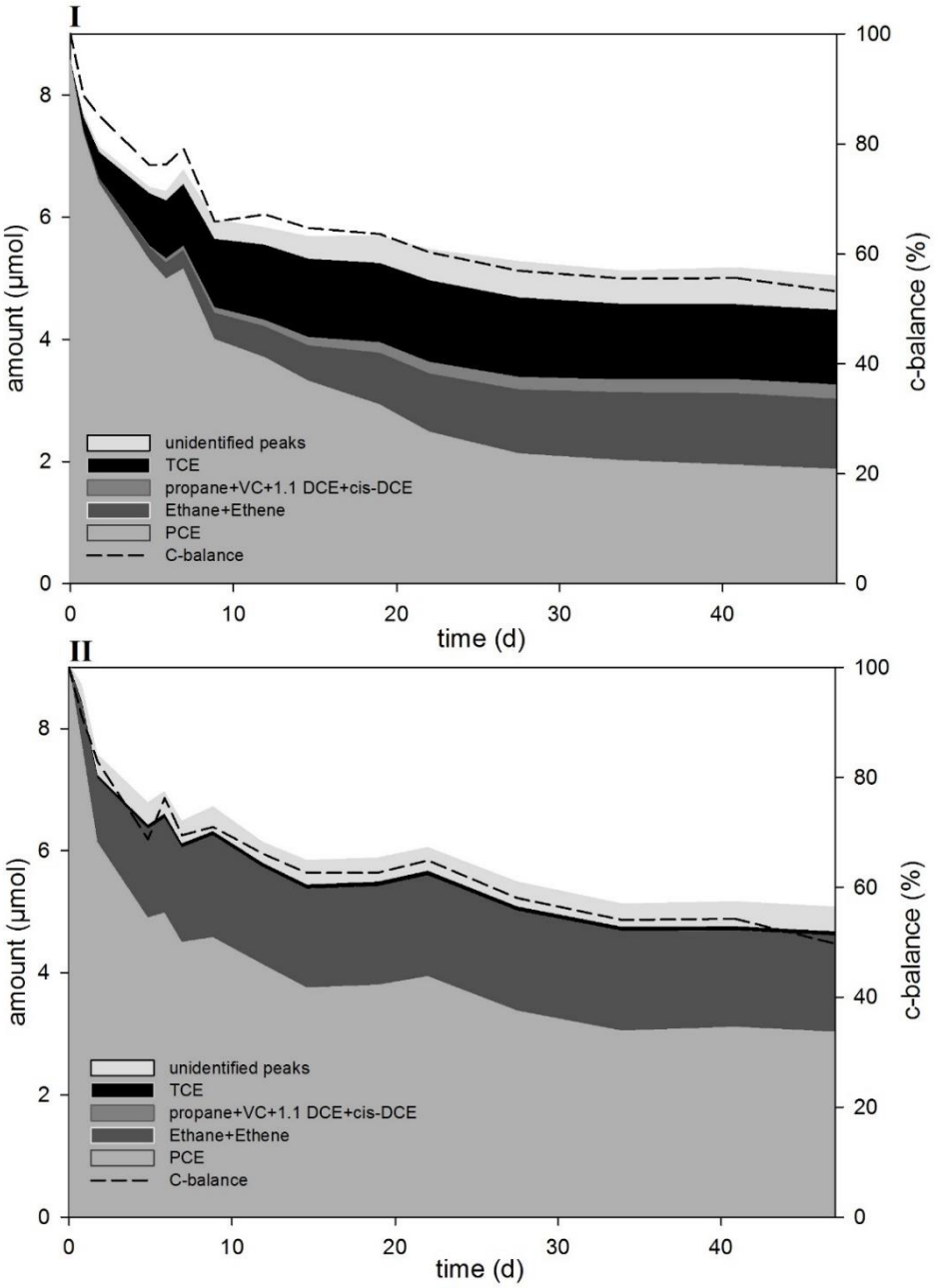

Figure 20: Summation of degradation and by-products (µmol) with unidentified peaks (shown in relation to other products) and carbon mass balances for samples with 380 mg L^{-1} RL (I) and 1 mg L^{-1} RL (II)

The carbon mass balance (dashed line in Figure 20) did not fit the overall sum of the amounts of PCE and degradation products because the initial measurement of the samples in the second repetition could not be evaluated. Therefore, the first measurement was neglected and the second measurement was accounted as starting values for the calculation of carbon mass balances.

There was no big difference in the measured pH values of the different treatments (Figure 21). The pH values were determined on day 0 after the preparation of the samples but before injection of the nZVI suspension, on day 1 after nearly 24 hours with nZVI and at the end of the experiment (day 48). In all samples containing nZVI, the pH values measured after nZVI injection stayed nearly the same over the whole time of the experiment and were around 7.31 ±0.14 (day 1) and 7.20 ±0.03 (day 48). Freshly measured samples on day 0 without nZVI showed a lower pH (6.21 ±0.13). The pH at the end of the experiment was almost the same for all the samples regardless of whether they contained nZVI or not (7.13 ±0.12).

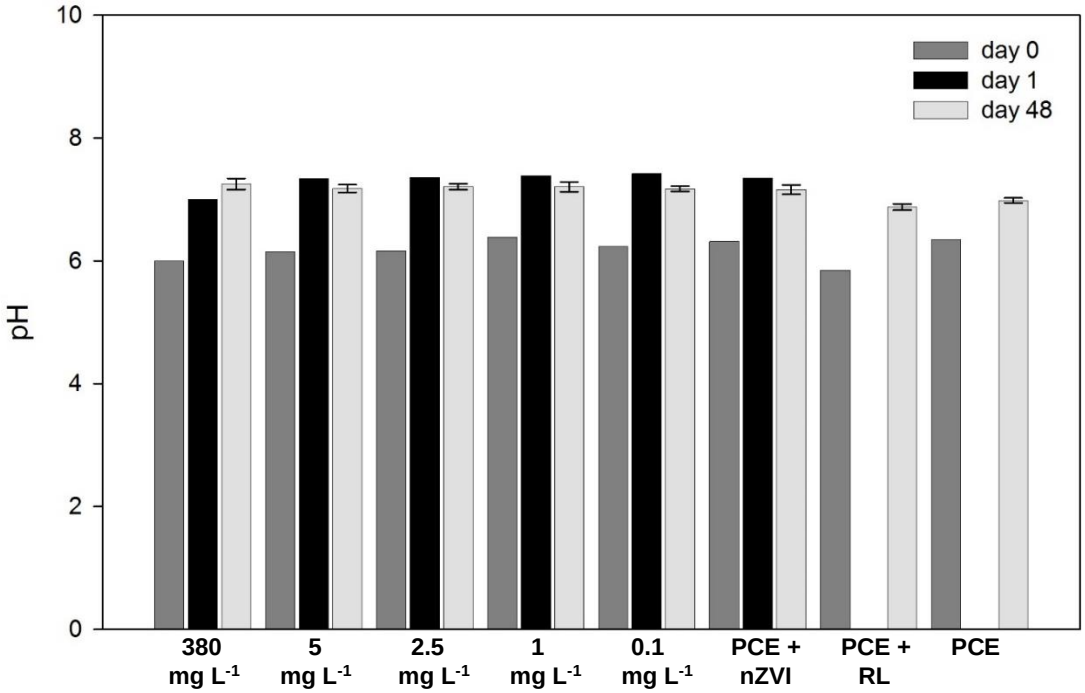

Figure 21: pH values of different samples on day 0 (without nZVI), day 1 (after 24 hours with nZVI) and at the end of the experiment on day 48 with standard deviation (*n=2*)

The ORP measurements done simultaneously with the pH measurements showed no constant value for the samples at a given time point but shifted in the ORP (decrease or increase over ORP measuring time). Samples were measured till the value was stable or after around three hours. Figure 22 shows measured ORP values of all samples at the beginning (I) and at the end (II) of the ORP measuring process. The lowest OPR value was measured for the treatment

with 2.5 mg L^{-1} RL with -302.7 mV_H on day 1 (with nZVI) at the end of the measuring process. ORPs in the beginning of the measuring process (I) on day 0 differed strongly from ORPs in the end of the measuring process (II). On day 1, after 24 hours with nZVI, when negative controls containing PCE and PCE + RL were not measured, the ORP of all other treatments was between 35.7 mV_H (380 mg L^{-1} RL) and -270 mV_H (2.5 mg L^{-1} RL) and differed not much from the ORP at the end of measuring (-65.1 mV_H for 380 mg L^{-1} and -302.7 mV_H for 2.5 mg L^{-1} RL).

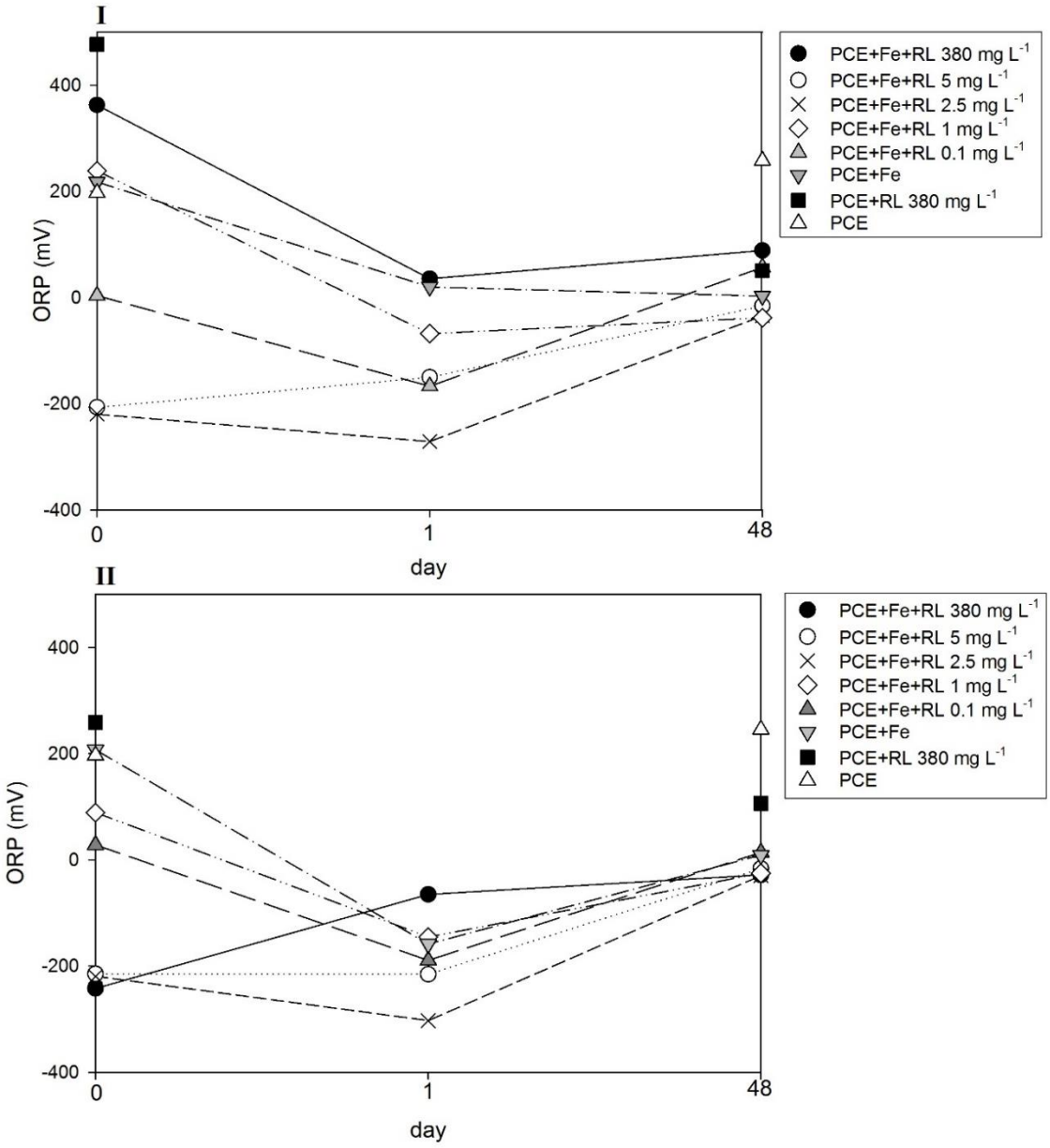

Figure 22: Measured values of ORP (mV_H) for all treatments on day 0 (without nZVI), day 1 (with nZVI) and at the end of the experiment on day 48 and the ORP in the beginning (I) of the OPR measuring process and in the end (II)

Also at the end of the experiment duration, ORPs except for negative control samples with PCE and PCE + RL, were all in the range of 89 mV_H (380 mg L^{-1} RL) to -34.1 mV_H (2.5 mg L^{-1} RL) at beginning of the measurement (Figure 22, I) and with an even narrower range of 13.9 mV_H (only PCE + nZVI) to -29.7 mV_H (2.5 mg L^{-1} RL) in the end of the ORP measurement (Figure 22, II). Negative controls with PCE were stable at around 200 mV_H for the time of the experiment and did not change much over the ORP measuring time. The ORP of the samples containing PCE + RL dropped over time from around 477 mV_H / 260 mV_H (beginning/ending of measurement) on day 0 to around 51 mV_H / 100 mV_H.

The volumetric measurements of the reference samples of the iron suspensions showed an Fe(0) content of 11.53 ±0.57 % for the first, 9.60 ±0.41 % for the second and 10.40 ±0.62 % for the third batch. The Fe(0) contents of the samples were calculated using these values of the different suspensions of the batches (1–3) and the gravimetrically determined added mass of iron (Table 14).

Table 14: Fe(0) content of samples of the different repetitions in g L^{-1} (*n=3*)

	380 mg L^{-1}	**5 mg L^{-1}**	**2.5 mg L^{-1}**	**1 mg L^{-1}**	**0.1 mg L^{-1}**	**PCE + nZVI**
repetition 1	1.274	1.300	1.170	1.248	1.248	1.248
repetition 2	1.152	1.128	1.128	1.128	1.176	1.152
repetition 3	1.274	1.300	1.170	1.248	1.248	1.248
mean	1.233	1.243	1.156	1.208	1.224	1.216
std. dev.	0.058	0.081	0.020	0.057	0.034	0.045
s.d. in %	4.7	6.5	1.7	4.7	2.8	3.7

The Fe(0) content of the iron suspension of the second batch was lower than the content of the other batches. The lower Fe(0) content in the suspension led to a decreased Fe(0) content in the samples of the second repetition compared to the other samples of 5-10 mg per vial (which translates to 10 to 20 % less Fe(0)).

Measurements of Fe(0) in the end of the sampling process showed that in most samples no Fe(0) was remaining. For the third repetition it was not possible to measure the Fe(0) content due to lack of time.

The total iron content of the samples was measured at the end of the experiment using AAS (Table 15). These measurements also showed a lower concentration of iron in the second repetition (except the sample with 2.5 mg L^{-1} RL).

Table 15: Content of total iron in the samples of the different repetitions in g L^{-1} (*n=3*)

	380 mg L^{-1}	**5 mg L^{-1}**	**2.5 mg L^{-1}**	**1 mg L^{-1}**	**0.1 mg L^{-1}**	**PCE + nZVI**
repetition 1	3.520	2.534	2.418	2.518	1.465	1.860
repetition 2	1.610	0.924	2.454	1.997	2.178	2.416
repetition 3	3.390	2.796	2.555	2.882	2.794	3.264
mean	2.840	2.085	2.476	2.466	2.146	2.513
std. dev.	0.871	0.828	0.058	0.363	0.543	0.577
s.d. in %	30.7	39.7	2.3	14.7	25.3	23.0

The electron efficiency of nZVI was calculated for PCE and H_2 (Figure 23). The electron efficiency for H_2 was close to 100 % for all the samples, ranging from 96.4 ±10.3 % (5 mg L^{-1} RL) up to 101.6 ±5.9 % (1 mg L^{-1} RL). The only exception was the treatment with 380 mg L^{-1} RL with a slightly lower H_2 electron efficiency of 89.3 ±6.8 %. In contrast, the PCE electron efficiencies were much lower. The samples showed a slight increase in PCE electron efficiency with decrease in rhamnolipid concentration from 1.20 ±0.15 % (380 mg L^{-1} RL) up to 1.39 ±0.14 % (0.1 mg L^{-1} RL). Opposed to that, the negative control with PCE + nZVI had the lowest PCE electron efficiency of 1.05 ±0.20 %. There was no significant difference (*p>0.05*) in neither the H_2 nor the PCE electron efficiencies of the different treatments.

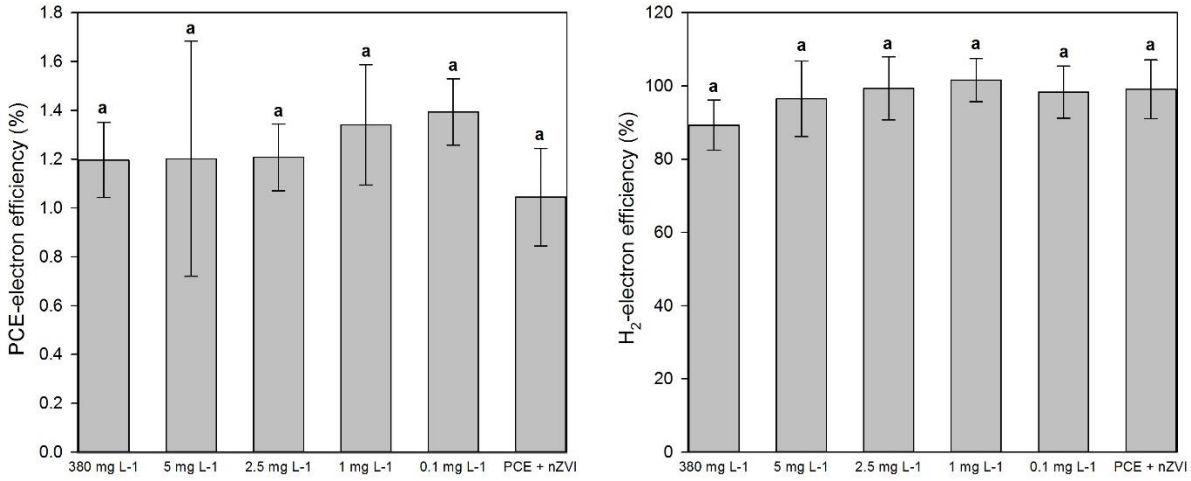

Figure 23: PCE electron efficiency (left) and H_2 electron efficiency (right) for all treatments (*n=3*)

3.4. Post-test regarding loss of PCE

The samples of the post-test with PCE + H_2O and PCE + H_2O + quartz sand also showed a loss of PCE over the time measured. The k_{obs} of the PCE loss of the post-test was compared to the k_{obs} of the samples of the negative control from the main experiment containing PCE (see Table 16).

Table 16: k_{obs} (h^{-1}) of the two treatments of the post-test and the negative control with PCE from the main experiment

	PCE + H_2O	**PCE + H_2O + quartz sand**	**PCE (main exp.)**
k_{obs}	8.79E-04	7.76E-04	5.71E-04
std. dev.	4.09E-04	1.17E-04	1.88E-04
s.d. in %	47	15	33

The loss in PCE of the post-test and of the control group of the main experiment was comparable (see Figure 24) and the k_{obs} for the loss did not differ significantly. As in the negative control of the main experiment, no degradation products were formed. There was no difference in the loss of PCE whether the samples contained quartz sand or not.

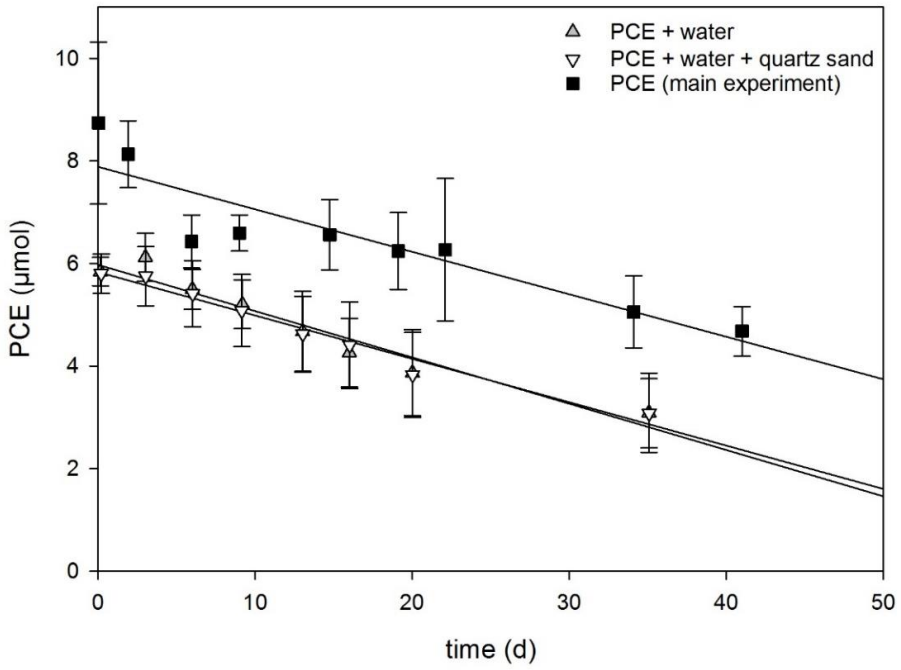

Figure 24: Loss of PCE (µmol) over time for the post-test containing PCE + H_2O and PCE + H_2O + quartz sand and the negative control with PCE from the main experiment (*n=3*)

The measurements on the GC-ECD of the aqueous phase done on the first four measuring points showed that the calculated aqueous concentration was higher than the measured aqueous concentration. The ratio of measured values on the GC-ECD to the aqueous values calculated from measured gaseous concentration on the GC-FID are listed in Table 17.

Table 17: Ratio of mg PCE in aqueous phase measured on GC-ECD to amount in aqueous phase calculated out of measured mg PCE in gaseous phase from GC-FID (*n= 3)*, QS = quartz sand

	day 0	**day 3**	**day 6**	**day 9**
PCE + H_2O	0.84 ±0.05	0.65 ±0.01	0.71 ±0.03	0.72 ±0.09
PCE + H_2O + QS	0.82 ±0.03	0.63 ±0.05	0.67 ±0.02	0.67 ±0.01

4. DISCUSSION

4.1. Pre-tests regarding the interaction of PCE and surfactant, foaming and iron particles

The aim of this first pre-test was to determine whether the PCE and the surfactant react with each other and degradation products are built. It showed that in the samples with saponin, PCE decreased but was not degraded as no degradation products could be found, so no reduction of PCE by surfactant took place. ALESSI & LI (2001) also concluded that HDTMA surfactant alone does not react with PCE because their negative control samples with HDTMA and PCE showed no loss in PCE. In contrast to the negative controls in the main experiment with only PCE, the one sample containing PCE and no surfactant was stable and showed no decrease in PCE. There seems to be some kind of interaction between surfactant and PCE regarding the decrease in all the samples with saponin or there also is an unspecific loss in PCE like in the samples of the main experiment.

The other pre-tests, done to visually observe the production and the collapse of the foam with and without nZVI and with different surfactant concentrations, showed that the samples containing surfactant above the CMC built up rather much foam after shaking them horizontally for 24 hours. The foam collapsed faster in the samples containing quartz sand. Thus, samples of the main experiment were prepared with quartz sand.

In the third pre-test, the foam in the samples with nZVI and surfactant above CMC was rather stable. It was assumed that it would be impossible to draw samples of PCE and its degradation products of the headspace if it was filled with foam because there would not be a gaseous phase were the compounds could equally diffuse. Even if only the water phase was fully covered with foam, it was expected that the foam interfered with the Henry constant and degassing substances would be hindered to enter the gas phase above. This concern was confirmed in the sample VVS 5 (with nZVI, high saponin concentration and quartz sand), where gas bubbles accumulated visibly at the interface of water and foam. As it took too long for the foam to collapse after shaking, it was concluded that the samples of the main experiment with RL should be put on the shaker standing upright and shaken like this to avoid formation of too stable foam.

The distribution of nZVI on the bottom of the sample vials, observable in the samples without quartz sand, showed that the saponin had an influence on the distribution of the nZVI particles. The particles in the samples with lower concentration followed gravity and accumulated at the sink at the walls of the vial whereas the particles in the sample with high saponin concentration were evenly distributed on the bottom of the vials. This would suggest an interaction of saponin with the nZVI particles. The saponin could have adsorbed on the iron particles and due to its non-ionic nature may have provided a good coverage of the particles. This could have hindered aggregation by providing steric hindrance. It can also be seen in the first picture (in Figure 12) taken immediately after taking the samples from the shaker that the nZVI in the sample with the lower saponin concentration (VVS 8) sedimented faster than in the sample with the higher saponin concentration (VVS 7). It could also be that the surfactant micelles present in the samples with the higher saponin concentration interacted with the nZVI particles. No precise conclusion can be drawn because there are no studies regarding the interaction of specifically saponin with nZVI.

4.2. Pre-test regarding production of H_2 by different iron particles

This pre-test showed that Nanofer Star particles were the most suitable particles to work with in the main experiment because of their fast reaction and the limited time frame of the experiment. Their production of H_2 stopped somewhere between day 22 and 35 indicating a fast reaction process confirmed by the high observed reaction rate constant. The samples remained tight as the internal standard fitted the calculated values.

It is noticeable that Hög AB as micrometer particle showed the highest reaction rate constant if related to the specific surface area of the iron particles (k_{SA}), about 30 times higher than Nanofer Star particles and 60 times higher than RNIP particles. This could be explained by the high Fe content of the Hög AB particles compared to RNIP and Nanofer Star particles. Also, although Nanofer Star particles stopped reacting, the amount of H_2 in RNIP and Hög AB samples increased between the last two measurement points suggesting that the reaction would have continued even after 98 days. Nanofer Star particles and RNIP particles show an almost similar and steeper curve than Hög AB particles in the first 9 days of the experiment. From this on, the production of H_2 from RNIP particles was slower and reached only 5,402 ±91 µmol overall. So, RNIP particles showed a decrease in reactivity after day 9, whereas Nanofer Star particles continued producing H_2 in the same speed until about 7,357 ±212 µmol. This would indicate that the Nanofer Star particles oxidize to a much high-

er rate than the RNIP particles (like observed by SCHÖFTNER et al., 2014). LIU et al. (2007) found a decrease in reactivity of the RNIP particles with TCE at later times if the concentration of TCE was high and attributed it to the formation of a passivating Fe-oxide layer. They also described a stop in production of H_2 at day 6 to 54 depending also on the concentration of TCE and a reactive lifetime of RNIP particles <10 d. The decrease in reaction rate of the RNIP particles with water can be attributed to their Fe_3O_4 shell which also makes some of the Fe(0) inaccessible (LIU et al., 2007). The stop in the production of H_2 from Nanofer Star particles between days 22 and 35 indicates that its oxidizing potential was used up. So, despite Nanofer Star and RNIP particles being two nanoscale particles, they behave differently due to their composition.

4.3. Batch experiment with rhamnolipid

The loss in measured PCE in the negative control groups with only PCE was not expected during experimental set-up. Therefore, the post-test was conducted to identify a possible cause. All values had to be corrected for this unspecific loss to not calculate much higher observed reaction rate constants and attribute it to a degradation of PCE by nZVI or interaction with RL.

4.3.1. Carbon mass balances

Carbon mass balances were achieved of 50 % to 62 % and were therefore low compared to other experiments, e.g. LIU et al. (2005), who reported carbon mass balances of 85-92 % or BHATTACHARJEE et al. (2016), who achieved carbon mass balances >90 %. The low carbon mass balances in this experiment are due to the large unspecific loss of PCE (and maybe other degradation products) in all the samples. Also, not all possible degradation and by-products of the reactions could be qualified (e.g. dichloroacetylene, chloroacetylene, trans-1,2-DCE). The increase in the amount of unidentified peaks indicates that these could be unidentified degradation products. Further, other by-products of the reaction like propylene, 1-butylene, 2-butylene, butane, 5-carbons and 6-carbons (LIU et al., 2005) which were not determined in this experiment could have caused these unidentified peaks.

4.3.2. Differences of the treatment with highest RL concentration

The treatment group that differed significantly from the other treatment groups (disregarding the negative controls with PCE + RL and PCE) was the one with the highest RL concentration with 380 mg L^{-1}. This treatment showed significant differences by having a higher decrease in

PCE, a higher $k_{obs22,PCE}$ and $k_{SA22,PCE}$ and a lower $k_{obs22,H2}$, $k_{SA,H2}$ and c_{22}/c_0 ratio.. It had a significantly higher amount of TCE and the production of ethene and ethane was lower. Propane, 1,1 DCE and cis-DCE were measured in small concentrations in contrast to the other treatments, where only a small amount of propane was found. Vinyl chloride was only detectable in a small amount in the control with only PCE + nZVI. Its calculated $k_{obs50\%,PCE}$ and the amount of H_2 produced (µmol) did not differ significantly from the other treatment groups.

4.3.3. Influence of RL on the degradation of PCE and production of H_2

The concentration of PCE in all the samples decreased till day 22 of the experiment and then remained constant. Therefore, the k_{obs} were calculated for the first 22 days. Contrary to the lag phase in TCE degradation by nZVI during the first four to five days observed by SCHÖFTNER et al. (2015), the PCE degradation started immediately. In most of the samples (16 out of 21 samples), 50 % of the PCE were degraded after 12 to 15 days of the experiment with the biggest decline in the first 7 days of the experiment (with PCE values corrected for unspecific loss). SCHÖFTNER et al. (2015) observed k_{SA} for TCE that was ten times the calculated $k_{SA22,PCE}$ of this experiment, but the unspecific loss of PCE in this study has to be accounted here. Further, their k_{SA} for the production of H_2 was a fourth of the $k_{SA22,H2}$ of the control with only PCE + nZVI.

The lower $k_{SA22,H2}$ for the treatment with the highest RL concentration compared to the negative control with PCE + nZVI and the treatments with the lower RL concentration suggests that the RL had an influence on the formation of H_2. It could be that the RL and the H^+ are competing for the same reactive sites and that some sites were blocked by RL. This would also explain why the overall amount of H_2 produced was lower in the samples with the highest RL concentration. BHATTACHARJEE et al. (2016) observed in their studies RL and Pd competing for the same reactive sites and RL deposition on nZVI inhibiting TCE degradation.

Measured H_2 and PCE electron efficiencies indicate that a large portion of released electrons from iron particles is reacting with water instead of the target contaminant. This is consistent with results from SCHÖFTNER et al. (2015), although their calculated PCE electron efficiencies were higher than in this study. The unspecific loss of PCE would contribute to lower PCE electron efficiencies. Also, they did not use quartz sand in their study and shaking was done differently. It seems the contaminant was more available for the nanoiron particles because of the better mixing and the more homogeneous conditions in their sample vials than in this study.

The most important factor for the reaction to take place is that the contaminant is near the surface of the nZVI or sorbed to the surface (ALESSI & LI, 2001; LORAINE, 2001). It could be that the different ingredients (nZVI particles, surfactant, PCE) were excluded because they were dispersed in the pores of the quartz sand and therefore could not react. The shaking of the flasks standing upright did offer only poor mixing of the ingredients compared to shaking them lying on the shaker. Two times the samples were shaken horizontally which led to an increase in pressure compared to the other days indicating a better mixing of the reactive substances and an increase in reaction rate.

4.3.4. Possible causes for the influence of surfactant on PCE degradation

The influence of a surfactant on the reductive dechlorination process may depend strongly on the charge of its polar head group. There are studies suggesting that the dechlorination rate is enhanced with cationic surfactant: ALESSI & LI (2001) showed that the dechlorination rate constant with ZVI increased by a factor of 3 in a solution with surfactant (HDTMA). The postgrafted surfactant-modified ZVI particles showed rate constants 12-19 times higher for HDTMA-modified ZVI than unmodified ZVI. Other studies compared different surfactants and as well found a positive influence of cationic surfactant while anionic and non-ionic surfactant were indifferent to or even inhibited the reaction (LORAINE, 2001; SHIN et al., 2008; LIANG et al., 2014). LORAINE (2001) further observed that non-ionic surfactant Triton X-100 enhanced PCE reduction rate but could not help degrade TCE. Another study by HARENDRA & VIPULANANDAN (2008) also suggest a positive influence of not only cationic but also non-ionic surfactant on degradation of PCE by bimetallic Fe-Ni particles. This indicates that the use of cationic (or non-ionic) surfactant is better suited to positively influence the reductive dechlorination process of PCE. But only a few biosurfactants are cationic and most of them are anionic or non-ionic (MULLIGAN, 2004). Also, it has to be considered that SHIN et al. (2008) did their experiments on the degradation of TCE and not PCE. TCE degradation was not enhanced in this study either. LIANG et al. (2014) used another contaminant (polybrominated diphenyl ethers) to study the impact on debromination. So, polarity of the headgroup of a surfactant cannot be seen as the major cause why surfactant alter the degradation of contaminants because of these studies although it could have an influence.

Some studies on the influence of surfactant were done with bi-metallic particles (e.g. BASNET et al., 2013; HARENDRA & VIPULANANDAN, 2008; HARENDRA & VIPULANANDAN, 2011; ZHANG et al., 2016; BHATTACHARJEE et al., 2016). BASNET et al. (2013) investigated the influence on transport and aggregation behaviour and observed good colloidal stability and

enhanced transport of Pd-nZVI particles with RL. Surfactants can also increase the degradation rate by promoting desorption of contaminant (ZHANG et al., 2016). HARENDRA & VIPULANANDAN (2011) used both, nZVI and Fe-Ni particles in their study and reported a positive influence of cationic surfactant (cetyltrimethylammonium bromide or CTAB) on degradation of PCE by both particle types. The nonionic surfactant Triton X-100 enhanced degradation of PCE with nZVI particles but performed not as good with Fe-Ni particles as the control with water. HARENDRA & VIPULANANDAN (2011) concluded that the difference was due to the size of the micelles with Triton X-100 having smaller micelles than CTAB. BHATTACHARJEE et al. (2016) also observed higher reaction rates with RL coated Pd-nZVI particles but an increase in surfactant loading resulted in a decrease in k_{obs}. They attributed the decrease in reaction rate to blocking of Pd sites by RL.

Other than NASSER (2012), who assigned the increase in conversion reaction of Cr(VI) to a decrease in aggregation of iron particles due to RL, HE & ZHAO (2007) observed an increase in degradation rate of TCE by carboxy methyl cellulose coated Pd-nZVI particles that was not directly proportional to the increase in specific surface area of the particles. The increase in TCE degradation was due to smaller particle sizes but there was an optimum carboxy methyl cellulose concentration at which further increase in concentration is believed to block reactive sites by adsorption. The size of carboxy methyl cellulose molecules influences the intensity of the repulsive forces and the steric hindrance. HE & ZHAO (2007) therefore suggest a stabilizer with both, hydrophobic and hydrophilic entities and a balanced molecular weight. Also, BHATTACHARJEE et al. (2016) reported a lack in correlation of aggregate sizes and degradation rates. They concluded that aggregate size appears to not be as important as the aggregate morphology of the nZVI particles.

ZHANG & MILLER (1995) stated that enhancement in hydrocarbon biodegradation is due to the structure of biosurfactant and not to the polarity of the head group. Rhamnolipids produced from P. aeruginosa are a mixture of anionic and non-ionic mono- and di-RL acids and methyl esters. ZHANG & MILLER (1995) showed that mono-RL have to be present in higher concentrations to stimulate biodegradation of alkanes and di-RL only in small concentrations to have the same effect. Also, di-RL methyl esters stimulated biodegradation for hexadecane and octadecane most and also helped disperse hexadecane more than di-RL acids. Although di-RL methyl esters are more effective in stimulating biodegradation they have to be mixed with di-RL acids because of their low water solubility. It is not clear, how many strains of Pseudomonas are able to produce RL methyl esters, although most strains produce mixed RL

(ZHANG & MILLER, 1995). This indicates that due to the natural diversity in the composition of RL, some components could be more helpful in increasing the degradation of contaminants than others and also the ratio of this different components in the surfactant mixture is important.

Another possible cause of increased contaminant degradation is that the surfactant sorbed to the iron particles increases the fractional organic carbon content and thus they serve as hydrophobic adsorption sites. The PCE will then partition into these hydrophobic sites and so gets in contact with the iron surface which would enhance degradation (ALESSI & LI, 2001). ALESSI & LI (2001) found that the rate of degradation of PCE by surfactant modified nZVI particles was relatively higher for particles modified with lower surfactant loading than that with higher surfactant loading and attributed this to the blocking of reaction sites.

It is also stated, that after the CMC of the surfactants was exceeded it is believed that PCE and TCE could be sequestered by micelles (LORAINE, 2001) or that PCE could partition into the micelles (ALESSI & LI, 2001). This would also explain the decrease in PCE without degradation products in the negative control with PCE + RL as a RL concentration above CMC was used. Regarding the influence of degradation of contaminant by nZVI because of micelles it could be that a high number of micelles in the solution can lead to a lower availability of PCE for nZVI because more PCE is inside of micelles (ALESSI & LI, 2001; LORAINE, 2001; ZHANG et al., 2011). It has to be considered that micelles may not be fully developed if the concentration is just reaching the CMC because part of the surfactant may be sorbed on the nanoparticles (ZHANG et al., 2011). In the micelles, nonpolar molecules can bind to the hydrophobic regions and they are transported with the micelles. On an active site, the reactant has to replace the surfactant or has to be within roughly one head group diameter of the surfactant for a successful electron transfer. It is possible for reactants trapped in micelles to be delivered to adsorbed surfactants on active sites or the micelle can join the adsorbed surfactants and so bring the reactants closer to each other (RUSLING, 1997). This suggests that even though the CMC is reached in the samples with the highest RL concentration, potential PCE in micelles can nevertheless interact with nZVI particles.

4.3.5. Influence of RL on degradation products and reaction pathway

More degradation products were found in the treatment with 380 mg L^{-1} than in the other treatments with PCE, RL and nZVI. They consisted of a higher amount of TCE and 1,1-DCE and cis-DCE were detected although the amount of ethane and ethene was lower. The high

amount of TCE would suggest that the reaction pathway in the treatment with 380 mg L^{-1} consisted mostly of hydrogenolysis of PCE which would contrast with the primary pathway used in reductive dechlorination by zero-valent iron, found by ARNOLDS & ROBERTS (2000) to be β-elimination. LORAINE (2001) also observed a higher concentration in TCE with the non-ionic surfactant Triton X-100 (TX) compared to the anionic surfactant sodium dodecyl sulfate (SDS) and the control group without surfactant. The calculated difference in the TCE yield for deionized water and TX increased with increasing surfactant concentration. As the observed change cannot be attributed to different absorption of TCE or PCE, LORAINE (2001) concluded that there must be an influence of TX on the reaction mechanism of PCE and that maybe TX has acted as H donor and the hydrogenolysis pathway was more important. LI et al. (2002) also observed a shift towards hydrogenolysis when using cationic surfactant (HDTMA) coated ZVI to degrade PCE. Although more TCE was produced, the overall rate of PCE and TCE degradation was still faster than in samples without surfactant (LI et al., 2002). This indicates that, opposed to this study, TCE decreases also in the presence of nZVI with cationic surfactant. As mentioned before, LORAINE (2001) observed that non-ionic surfactant (TX) enhanced PCE reduction rate but could not help degrade TCE. So, it is possible that either the charge of the polar group or the chemical structure of the surfactant (comparing HDTMA and TX) is interfering with the degradation of TCE. Maybe a difference in sorption of the different surfactants on the nZVI particles leads to blocking reactive sites which TCE would use. It could also be that the less hydrophobic and more soluble TCE will partition less to surfactant admicelles than PCE (ALESSI & LI, 2001). Therefore, the enhancement in TCE degradation with surfactant coated ZVI particles might be less than the enhancement in PCE degradation. LI et al. (2006) further confirmed the change in dechlorination pathway conducting column studies with surface-modified nZVI particles and PCE. They concluded that desorption of TCE would be more readily and so the amount of TCE in the aqueous phase would be greater than the amount of TCE in the sorbed phase which would inhibit the reaction of TCE with nZVI.

There was no ethyne found in all the different treatments like in the experiments conducted by SCHÖFTNER et al. (2015). LIU et al. (2005) did also not detect ethyne in their samples but observed that vinyl chloride and cis-DCE disappeared quickly. Contrary, in this experiment, their amount stayed stable over time in the samples with the highest RL concentration which could be due to the exhausted reduction potential of the iron particles or because of the same reasons why there was no further degradation of produced TCE.

4.3.6. pH and ORP measurements

The pH measurements on day 0 (without nZVI) showed a lower pH of around 6 in all the samples whether they contained nZVI or not. After addition of the nanoiron suspension, the pH was stable in all the samples from day 1 to day 48. This implicates that the added HEPES buffer was enough and guaranteed a stable pH over the time of the experiment.

It is not clear why the ORP measurements did not show a definite stable value for one sample. Shifting ORP values while measuring the filtrated solutions of the samples would indicate redox reactions still going on in the solution. The solution was passed through a syringe filter <0.2 µm (= <200 nm) which was maybe too wide to filter all the nZVI particles out of the solution. This would explain why the ORP values differed not so much between beginning and end of ORP measurements on day 48 than the values of day 1 (first measurement with nZVI). Then again, also the treatment with only PCE + RL differed on day 0 of the measurement. The first treatments measured on each day (treatment with 380 mg L^{-1} RL, with 1 mg L^{-1} RL and negative control with PCE + RL) showed the highest difference in ORP over the measuring process (beginning and ending). This implies an error in preparing the mobile probe before measuring the samples. Also, pre-conditioning of the mobile probe for reducing conditions would be reasonable in the future to avoid long set-up times. The increase in ORP from day 1 to day 48 showed that the iron was oxidized during the experiment. It is not clear why there was a decrease in ORP in the treatment with PCE + RL from day 0 to day 48. The measured ORP was never as low as measured ORP values by SCHÖFTNER et al. (2015).

4.4. Post-test regarding loss of PCE

As other studies (e.g. ZHANG & WANG, 1997; ALESSI & LI, 2001; SCHÖFTNER et al., 2015) did not report a loss of PCE in control groups containing PCE and surfactant or only PCE, the post-test was conducted for further investigation.

The post-test confirmed the loss of PCE observed in the negative control with only PCE of the main experiment. The calculated k_{obs} for the post-test samples were in the same range as the k_{obs} of PCE in the main experiment. There was also no difference in PCE loss whether the samples contained quartz sand or not. The amount of H_2 plateaued after around 10 days in most samples and remained almost constant for the rest of the experiment till day 48. If the sample vials were not tight, H_2 as the smallest substance would have vanished first. Then again, it could be that the production of H_2 never stopped and because of its constant loss it seemed as if the samples were tight. Also, other degradation and by-products of the experi-

ment which remained constant over time (e.g. ethene and ethane) could have been lost like this. But as the measured amount of CH_4 as internal standard fitted the calculated amount, this explanation can be excluded.

The loss can also not be explained by the use of the quartz sand as the samples without quartz sand did also lose PCE in the same scale over time.

One possible reason for the loss could be that the PCE diffused into the chlorobutyl-isoprene blend stoppers of the vials. This would explain why SCHÖFTNER et al. (2015) did not observe the same loss for their samples although the experiments were similar (albeit no use of quartz sand and surfactant). The difference is that they used vials equipped with another sealing mechanism (Miniinert valves). Miniinert valves have integrated resealable valves to eliminate septum-boring. The chlorobutyl-isoprene blend stoppers used in these experiments are provided with a PTFE sealing on their underside which was perforated by the needles of the syringes for sampling. So it is possible that the PCE and maybe also some other degradation or by-products may have diffused into the stoppers. However, the one negative control sample of the pre-test with only saponin and PCE and glass beads did not show the same decline although the stoppers used were the same. But as there were no replicates made in the first pre-tests it is difficult to make assertions with only this one sample. Also, there were other differences to the main experiment: the samples contained (washed) glass beads instead of quartz sand and saponin as surfactant as opposed to rhamnolipid. Saponin is a non-ionic surfactant whereas rhamnolipid is anionic. What also differed was the PCE stock solution with acetone used in the pre-test. Acetone as solubilizer was not present in the samples of the main experiment but it is not reasonable how this could influence the measured PCE. Another difference from the main experiment was that the pre-test was shaken for 24 hours and then the samples rested for 24 hours before measuring. In this time span the samples had more time to reach equilibrium conditions than the samples of the main experiment as they rested only for 5-6 hours before measuring. Opposing to this, SCHÖFTNER et al. (2015) conducted experiments and concluded that 1 hour of resting is enough for the volatile substances to reach equilibrium.

Calculations to verify the starting concentration in the main experiment show that the overall amount of PCE (measured gaseous amount on GC-FID and calculated amount of aqueous phase) fitted the calculated desired starting concentration by 100 ±6 % for the first two repetitions of the main experiment. For the third repetition, the predicted initial concentration was around 33 % lower than the measured concentration. This would indicate an error in the ex-

perimental set-up of the third repetition. Regarding the calculation of the concentration in the samples it is interesting to notice that the aqueous concentrations of PCE measured for the samples of the post-test on the GC-ECD were not congruent with the calculated aqueous concentration via the Henry constant out of the gaseous concentration measured on the GC-FID. The measured values of PCE detected on the ECD were lower by one fifth for the starting measurements and by around one third at measurements on day 9 for both different treatments (with and without quartz sand). This would suggest that the overall PCE concentration in the samples (aqueous and gaseous phase) would be even lower than calculated. As the difference in measured and calculated values grows larger over time, it would suggest influence of measurements that are falsely calculated. Maybe the sampling and withdrawal of gaseous phase and resulting negative pressure interfered with the equilibrium conditions and Henry's constant was not applicable under these circumstances. Further experiments have to be conducted to investigate a possible influence of the calculations.

4.5. Experimental set up and method

Regarding the duration of the batch experiment it can be seen in the pre-tests that were done to observe the formation of H_2, that the reactivity of Nanofer Star particles ends at around day 22. This would suggest that this would be a reasonable long enough time span for further experiments. So, measuring the main experiment for 48 days was too long and the results of the measurements underline this as the decline in PCE ended around day 22. Also, the production of the degradation products and by-products, although produced slower in the treatment with the highest RL concentration, stopped at this point.

As there was no auto sampler, the samples had to be injected manually. The time span for measuring one sample and the cool down of the detector took around 30 minutes. With measuring standards beforehand, the number of treatments that could be done in the experiment was limited by the daily available measuring time. Otherwise, including another treatment containing only rhamnolipid and nZVI as negative control would have been desirable to see a possible interaction between the nZVI particles and the surfactant without contaminant.

It was good that the replicates were done at different time points so that the variation due to the new mixing of nZVI slurry and the new set of experiments was between the replicates and not between the different treatment groups.

Most of the studies investigating the effect of surfactants on contaminant degradation were not conducted as this study was done. NASSER (2012) did not use purchased nZVI particles but self-produced particles and the surfactant was added in the manufacturing process of the nZVI particles ("pregrafting" according to BHATTACHARJEE et al., 2016). Also, in other studies (e.g. ALESSI & LI, 2001; BASNET et al., 2013; BHATTACHARJEE et al., 2016), the nZVI-slurry was equilibrated with the surfactant solution to allow the surface modifiers to adsorb onto the surface of the nZVI particles ("postgrafting" according to BHATTACHARJEE et al., 2016). Only in some studies (e.g. LORAINE, 2001; HARENDRA & VIPULANANDAN, 2008; ZHANG et al., 2011), the surfactant was added to the solution afterwards like in this study. ALESSI & LI (2001) also stated that an enhanced electron transfer from ZVI to PCE was observed when the ZVI was postgrafted with the surfactant compared to when the ZVI and surfactant were just mixed. BHATTACHARJEE et al. (2016) reported that postgrafted nZVI particles with excess rhamnolipid achieved only 20% of reduction of TCE compared to postgrafted particles without excess RL in solution. So maybe it would have been better to not only mix the surfactant to the solution but to add it before. Then, the surfactant solution and the nZVI should equilibrate for some time and the supernatant with unadsorbed surface modifier should be decanted before continuing with the experiments (postgrafting like described in BHATTACHARJEE et al., 2016).

The samples had to be put on the shaker upright and were shaken vertically. Another option for shaking was not possible because the produced foam would have interfered with the measurement of PCE and its degradation and by products. The results indicate that this led to poor mixing of the reactive substances and negatively influenced the degradation reaction so vertical shaking of the samples would guarantee more homogenous test conditions. The horizontal shaking of the samples (1 hour on day 5 after measuring and around 68 hours after day 15) led to an increase of pressure in the samples with the highest RL concentration. For the samples with lower RL concentration and the control with only PCE + nZVI the influence is not as clearly stateable as pressure was decreasing at this point and stopped in most samples around day 7. The increase in the samples with the highest RL concentration suggest that better mixing led to faster reactions taking place. As it is not possible to shake the samples with surfactant as thoroughly because of the production of foam, maybe it would be good to shake them horizontally at least for some time (e.g. 2 hours) after each measurement. Then they could be shaken vertically at night so that the foam can break down entirely before measuring

them again. This would ensure better mixing of substances. But, on the other hand, in the field, also no mixing mechanism can be applied.

Although there should have been enough nZVI in the samples to degrade the PCE, the degradation stopped at around day 22 indicating that the Nanofer Star particles were fully oxidized. The low PCE electron efficiency indicates that most of the nanoparticles reacted with water and not with the contaminant or its degradation products. So due to the large portion of nZVI reacting with water or the inaccessibility of contaminant due to the quartz sand it could be that there was not enough nZVI in the samples to degrade PCE and its chlorinated degradation products.

4.6. Materials

The standard PCE stock solution used in other experiments is one containing PCE and acetone as solubilizer (see pre-tests with PCE) to increase the dissolved PCE concentration. As it was not desirable to also have acetone in the samples with the surfactant, a new stock solution was prepared without acetone. The concentration was set to one third of the limit of solubility of PCE to guarantee the complete dissolution of PCE. It was selected because the PCE had to be completely dissolved without a solubilizing agent to attribute a possible influence on degradation by RL to the smaller particle size of the nanoiron and not to RL acting as solubilizing agent. The dissolution should have been complete, as there was no PCE phase visible in the stock solution flasks filled with MQ water. To get the PCE concentration needed in the sample vials, the PCE stock solution had to be opened and pipetted into the vials. This was done in the glove box. Although it was assumed that because of the volatility of the PCE it would lead to a loss of PCE while pipetting and sealing the vials, the initial measurements of PCE on the GC showed that the measured starting concentrations fitted the calculated starting concentration.

Also, maybe quartz sand should be treated before using it in the experiments. There could have been small organic fractions which could interact with the PCE and the surfactant by acting as adsorbing agents. BASNET et al. (2013) acid washed sand to remove metallic impurities and baked it for 6 h at 800 °C to remove organic impurities. This should be considered in further studies conducted with quartz sand.

The use of HEPES is necessary to guarantee a stable pH around 7.5 due to the production of hydroxide in the reductive dechlorination of PCE by nZVI. Although HEPES as hydrogen ion

buffer is one of "Good's buffer" (GOOD et al., 1966) and therefore should be chemically stable and inert to biochemical reactions, it is possible that nZVI also reacts with the HEPES buffer. There was no research found on the interaction of buffer and nZVI but nZVI is acting as strong reducing agent so an interaction cannot be excluded. Also, interference with experiments by buffers like HEPES was observed in other studies (e.g. BAKER et al., 2007). HEPES buffer oxidation is possible but oxidation of buffer is slow so this should not lead to significant influence on experiments (ZHAO & CHASTEEN, 2015). FERREIRA et al. (2015) suggest the testing of different buffers in an experiment to detect a possible influence of buffer on the reactions but also recommend to use HEPES.

Rhamnolipid was chosen for the experiments as it is a biosurfactant that is biodegradable under different environmental conditions (see chapter 1.3.1). The problem with using other industrially manufactured surfactants would be the concern about their fate if injected into the subsoil. Even if the remediation is successful this could lead to contamination of the groundwater or soil with another substance that is not eco-friendly or not biodegradable or maybe just biodegradable under certain conditions (most studies conducted investigating the biodegradation of surfactants are done under aerobic conditions according to MOHAN et al., 2006). If other substances are used for remediation of contaminated sites it is important to consider their potential risks as well and the application of potential harmful substances should be avoided. For the same reason, no bimetallic particles were used in this study. Despite their good performance, environmental concerns arise if substances like Ni or Pd are brought into the groundwater.

5. CONCLUSION

The use of nanoscale zero-valent iron to remediate chlorinated hydrocarbons looks promising: Nanoscale ZVI shows rather good results in batch experiments degrading contaminants efficiently, fast and effectively and producing desired non-hazardous end products of dechlorination like ethene and ethane while avoiding toxic intermediates. It can be used to remediate the source zone of a contamination and it can be applied in situ. Although there is research on nanoscale zero-valent iron for quite some time now, there are no adequate solutions for the biggest problems encountered when using nZVI for remediation: the loss of electrons due to the reaction of nZVI with water and other substances and not with the desired contaminant, the passivation of nZVI surface because of the formation of an oxide layer, their aggregation and their low transport range. There are different approaches using bi-metallic particles, surfactants, solvents and coatings but there is no solution which would address all problems.

In this study with RL it could be seen that the observed degradation rate constant of PCE of the samples with the lowest RL concentration (0.1 mg L^{-1}) was significantly higher than the control with only PCE + nZVI. Moreover, a significant difference was found in the degradation of PCE of the samples with the highest RL concentration (above CMC): More PCE was degraded with RL but it does not seem this was due to less aggregation of the particles but a shift in degradation mechanism. Also, less nZVI particles in the treatment with the highest RL concentration reacted with water which would be desired for the dechlorination. But the shift in degradation mechanism led to an increase in formation and accumulation of TCE and in a lower amount of desired end products of the dechlorination process. Regarding this result, the use of RL above CMC would not be useful to remediate contaminated aquifers because it would only cause a shift in hazardous contaminant from PCE to TCE. The significant difference of k_{SA} for PCE of the treatment with the lowest RL concentration compared to the negative control with only PCE + nZVI would suggest a positive influence of a low RL concentration. To further investigate this positive influence, an increase in the number of samples with lower RL concentrations would be useful to confirm statistical differences. In further research, it could also be tested if the RL could be added to the nZVI particles when the suspension is made rather than just adding the surfactant solution (postgrafting). Also, another experimental set-up should be used to avoid the large unspecific loss in PCE. More research is needed to better understand the mechanisms and interactions of surfactant with nZVI particles and with the contaminant.

REFERENCES

ALESSI, D.; LI, Z. (2001): *Synergistic Effect of Cationic Surfactants on Perchloroethylene Degradation by Zero-Valent Iron.* Environmental Science & Technology 35: 3713-3717.

ARNOLD, W.; ROBERTS, A. L. (2000): *Pathways and Kinetics of Chlorinated Ethylene and Chlorinated Acetylene Reaction with Fe(0) Particles.* Environmental Science & Technology 34: 1794-1805.

ATKINS, P.; DE PAULA, J. (2006): *Atkins' Physical Chemistry*. 8th Edition. Great Britain: Oxford University Press.

ATSDR (2014): *Draft: Toxicological Profile for Tetrachloroethylene.* U.S. Department of health and human services. Agency for Toxic Substances and Disease Registry. online: http://www.atsdr.cdc.gov/toxprofiles/TP.asp?id=265&tid=48 (08.06.2017)

BAKER, C. J.; MOCK, N. M.; ROBERTS, D. P.; DEAHL, K. L.; HAPEMAN, C. J.; SCHMIDT, W. F.; KOCHANSKY, J. (2007): *Interference by Mes [2-(4-morpholino)ethanesulfonic acid] and related buffers with phenolic oxidation by peroxidase.* Free Radical Biology & Medicine 43: 1322-1327.

BASNET, M.; GHOSHAL, S.; TUFENKJI, N. (2013): *Rhamnolipid Biosurfactant and Soy Protein Act as Effective Stabilizers in the Aggregation and Transport of Palladium-Doped Zero-valent Iron Nanoparticles in Saturated Porous Media.* Environmental Science & Technology 47: 13355-13364.

BHATTACHARJEE, S.; BASNET, M.; TUFENKJI, N.; GHOSHAL, S. (2016): *Effects of Rhamnolipid and Carboxymethylcellulose Coatings on Reactivity of Palladium-Doped Nanoscale Zerovalent Iron Particles*. Environmental Science & Technology 50: 1812-1820.

DE BOER, C.; BRAUN, J.; KLAAS, N. (2009): *Anwendung nanoskaliger Eisenkolloide zur In-Situ-Sanierung anthropogener CKW-Kontaminationen im Untergrund.* Abschlussbericht. Universität Stuttgart, Versuchseinrichtung zur Grundwasser- und Altlastensanierung (VEGAS). online: http://www.iws.uni-stuttgart.de/publikationen/vegas/Abschlussbericht_NANO_BUT_Jan2009.pdf (08.06.2017)

DÖRRIE, T.; LÄNGERT-MÜHLEGGER, H. (2010): *Technologiequickscan: In-situ-Sanierungstechnologien.* Wien: Österreichischer Verein für Altlastenmanagement (ÖVA). online: http://www.altlastenmanagement.at/home/2013/08/29/410/ (08.06.2017)

FENT, K. (2013): *Ökotoxikologie. Umweltchemie – Toxikologie – Ökologie*. 4th edition. Stuttgart: Georg Thieme Verlag KG

FERREIRA, C. M. H.; PINTO, I. S. S.; SOARES, E. V.; SOARES, H. M. V. M. (2015): *(Un)suitability of the use of pH buffers in biological, biochemical and environmental studies and its interaction with metal...* . The Royal Society of Chemistry 5: 30989-31003.

GOOD, N. E.; WINGET, G. D.; WINTER, W.; CONNOLLY, T. N.; IZAWA, S.; SINGH, R. M. M. (1966): *Hydrogen ion buffers for biological research*. Biochemistry 5 (2): 467-477.

GOSSETT, J. M. (1987): *Measurement of Henry's law constants for C1 and C2 chlorinated hydrocarbons.* Environmental Science & Technology 21: 202-208.

GRANDEL, S.; DAHMKE, A. (2008): *Leitfaden: Natürliche Schadstoffminderung bei LCKW-kontaminierten Standorten: Methoden, Empfehlungen und Hinweise zur Untersuchung und Beurteilung.* KORA-Themenverbund 3. Chemische Industrie, Metallverarbeitung. Christian-Albrechts-Universität zu Kiel, Institut für Geowissenschaften, Abt. Angewandte Geologie. online: http://www.natural-attenuation.de/download.html (08.06.2017)

GRANZIN, S.; VALTL, M. (2016): *Verdachtsflächenkataster und Altlastenatlas*. Stand: 1. Jänner 2016. Wien: Umweltbundesamt GmbH. online: http://www.umweltbundesamt.at/fileadmin/site/publikationen/REP0567.pdf (08.06.2017)

GUAN, X.; SUN, Y.; QIN, H.; LI, J.; LO, I. M C.; HE, D.; DONG, H. (2015): *The limitations of applying zero-valent iron technology in contaminants sequestration and the corresponding countermeasures: The development in zero-valent iron technology in the last two decades (1994-2014) – Review.* Water Research 75: 224-248.

HARENDRA, S.; VIPULANANDAN, C. (2008): *Degradation of high concentrations of PCE solubilized in SDS and biosurfactant with Fe/Ni bi-metallic particles.* Colloids and Surfaces A: Physicochemical and Engineering Aspects 322: 6-13.

HARENDRA, S.; VIPULANANDAN, C. (2011): *Solubilization and degradation of perchloroethylene (PCE) in cationic and nonionic surfactant solutions.* Journal of Environmental Sciences 23 (8): 1240-1248.

HE, F.; ZHAO, D. (2007): *Manipulating the Size and Dispersibility of Zerovalent Iron Nanoparticles by Use of Carboxymethyl Cellulose Stabilizers.* Environmental Science & Technology 41: 6216-6221.

HEALTH CANADA (1993): *Canadian Environmental Protection Act: Tetrachloroethylene. Priority substances list assessment report.* online: http://www.hc-sc.gc.ca/ewh-semt/alt_formats/hecs-sesc/pdf/pubs/contaminants/psl1-lsp1/tetrachloroethylene/tetrachloroethylene-eng.pdf (08.06.2017)

LI, Z.; WILLMS, C.; ZHANG, P.; BOWMAN, R. S. (2002): *Rate and pathway changes in PCE dechlorination by zero-valent iron in the presence of cationic surfactant.* In: GAVASKAR, A.R.; CHEN, A.S.C. (Eds.): *Remediation of Chlorinated and Recalcitrant Compounds - 2002. Proceedings of the Third International Conference on Remediation of Chlorinated and Recalcitrant Compounds (Monterey, CA; May 2002).* Columbus (OH): Battelle Press

LI, Z.; WILLMS, C.; ALLEY, J.; ZHANG, P.; BOWMAN, R. S. (2006): *A shift in pathway of iron-mediated perchloroethylene reduction in the presence of sorbed surfactant – A column study.* Water Research 40: 3811-3819.

LIANG, D.-W.; YANG, Y.-H.; XU, W.-W.; PENG, S.-K.; LU, S.-F.; XIANG, Y. (2014): *Nonionic surfactant greatly enhances the reductive debromination of polybrominated diphenyl ethers by nanoscale zero-valent iron: Mechanism and kinetics.* Journal of Hazardous Materials 278: 592-596.

LIDE, D. R.; FREDERIKSE, H. P. R. (1995): *CRC Handbook of Chemistry and Physics*. 76th Edition. Boca Raton: CRC Press, Inc.

LIU, Y.; LOWRY, G.V. (2006): *Effect of Particle Age (Fe0 content) and Solution pH On NZVI Reactivity: H2 Evolution and TCE Dechlorination.* Environmental Science & Technology 40: 6085-6090.

LIU, Y.; MAJETICH, S.; TILTON, R. D.; SHOLL, D. S.; LOWRY, G. V. (2005): *TCE Dechlorination Rates, Pathways, and Efficiency of Nanoscale Iron Particles with Different Properties*. Environmental Science & Technology 39: 1338-1345.

LIU, Y.; PHENRAT, T.; LOWRY, G. (2007): *Effect of TCE Concentration and Dissolved Groundwater Solutes on NZVI-Promoted TCE Dechlorination and H2 Evolution.* Environmental Science & Technology 41: 7881-7887.

LORAINE, A.G. (2001): *Effects of alcohols, anionic and nonionic surfactants on the reduction of PCE and TCE by zero-valent iron.* Water Research 35 (6): 1453-1460.

MARTENS, S.; EGGERS, B.; EVERTZ, T. (2010): *Untersuchung des Einsatzes von Nanomaterialien im Umweltschutz*. Dessau-Roßlau: Umweltbundesamt. online: http://www.umweltbundesamt.de/uba-infomedien/mysql_medien.php?anfrage=Kennummer&Suchwort=3778 (08.06.2017)

MOHAN, P. K.; NAKHLA, G.; YANFUL, E. K. (2006): *Biokinetics of biodegradation of surfactants under aerobic, anoxic and anaerobic conditions*. Water Research 40: 533-540.

MORTIMER, C. E.; MÜLLER, U. (2008): *Chemie: Das Basiswissen der Chemie*. 8th Edition. Stuttgart: Georg Thieme Verlag

MULLIGAN, C. N. (2005): *Environmental applications for biosurfactants.* Environmental Pollution 133: 183–198.

NASSER, F. (2012): *Conversion of Toxic Hexavalent Chromium to Trivalent Chromium by Rhamnolipid Stabilized Zero Valent Iron Nanoparticles*. Masterthesis at the University of Birmingham. online: http://etheses.bham.ac.uk/4347/1/Nasser13PhD.pdf (08.06.2017)

NOORDMAN, W. H.; WACHTER, J. H. J.; DE BOER, G. J.; JANSSEN, D. B. (2002): *The enhancement by surfactants of hexadecane degradation by Pseudomonas aeruginosa varies with substrate availability*. Journal of Biotechnology 94: 195-212.

NOUBACTEP, C. (2013): *Relevant Reducing Agents in Remediation Fe 0/H 2 O Systems.* CLEAN - Soil Air Water 41 (5): May 2013.

NRC (NATIONAL RESEARCH COUNCIL), (1994): *Alternatives for Ground Water Cleanup.* Washington, D.C.: National Academy Press. online: http://www.nap.edu/catalog/2311/alternatives-for-ground-water-cleanup (08.06.2017)

O'HANNESIN, S.F.; GILLHAM, R.W. (1992): *A permeable reaction wall for in situ degradation of halogenated organic compounds.* The 45th Canadian Geotechnical Society Conference, 25-28. October 1992, Toronto, Ontario.

PIVETZ, B.; KEELEY, A.; WEBER, E.; WEAVER, J.; WILSON, J.; MA, C. (2013): *Ground Water Issue Paper: Synthesis report on state of understanding of chlorinated solvent transformation*. United States Environmental Protection Agency. online: https://nepis.epa.gov/Exe/ZyPDF.cgi/P100JDPP.PDF?Dockey=P100JDPP.PDF (08.06.2017)

RADHAWA, K. K. S.; RAHMAN, P. K. S. M. (2014): *Rhamnolipid biosurfactants - past, present, and future scenario of global market.* Frontiers in Microbiology 5: Article 454.

REICHL, A. (1995): *Messung und Korrelierung von Gaslöslichkeiten halogenierter Kohlenwasserstoffe*. PhD thesis, Technische Universität Berlin, Germany.

ROBERTS, A. L.; TOTTEN, L. A.; ARNOLD, W.; BURRIS, D. R.; CAMPBELL, T. J. (1996): *Reductive Elimination of Chlorinated Ethylenes by Zero-Valent Metals.* Environmental Science & Technology 30 (8): 2654-2659.

ROBINSON, K. G.; GHOSH, M. M.; SHI, Z. (1996): *Mineralization enhancement of non-aqueous phase and soil-bound PCB using biosurfactant.* Water Science and Technology 24 (7-8): 303-309.

RUCKENSTEIN, E.; NAGARAJAN, R. (1975): *Critical Micelle Concentration. A Transition Point for Micellar Size Distribution.* The Journal of Physical Chemistry 79 (24): 2622-2626.

RUSLING, J. F. (1997): Molecular aspects of electron transfer at electrodes in micellar solutions. Colloids and Surfaces 123-124: 81-88.

SALE, T.; NEWELL, C.; STROO, H.; HINCHEE, R.; JOHNSON, P. (2008): *Frequently Asked Questions Regarding Management of Chlorinated Solvents in Soils and Groundwater.* Developed for the Environmental Security Technology Certification Program (ESTCP). Department of Defense (DoD). United States of America. online: https://www.serdp-estcp.org/content/download/8190/100865/version/1/file/FAQ-ChlorinatedSolvents-ER-200530.pdf (08.06.2017)

SANDER, R. (1999): *Compilation of Henry's Law Constants for Inorganic and Organic Species of Potential Importance in Environmental Chemistry.* Air Chemistry Department, Max-Planck Institute of Chemistry, Mainz.

SANDER, R. (2015): *Compilation of Henry's law constants (version 4.0) for water as solvent.* Atmospheric Chemistry and Physics 15 (8): 4399-4981.

SCHÖFTNER, P.; WALDNER, G.; REICHENAUER, T. G. (2014): *Projekt NanoSan: Schadstoffabbau und Reaktivität von nanopartikulärem Eisen*. Oral presentation on 26.02.2014: *Öffentliche Informationsveranstaltung: Einsatz von Nanopartikeln in der in situ Grundwassersanierung.* Vienna*:* Kommunalkredit Public Consulting GmbH.

SCHÖFTNER, P.; WALDNER, G.; LOTTERMOSER, W.; STÖGER-POLLACH, M.; FREITAG, P.; REICHENAUER, T. G. (2015): *Electron efficiency of nZVI does not change with variation of environmental parameters*. Science of The Total Environment 535: 69-78.

SCHRICK, B.; HYDUTSKY, B. W.; BLOUGH, J. L.; MALLOUK, T. E. (2004): *Delivery Vehicles for Zerovalent Metal Nanoparticles in Soil and Groundwater*. Chemistry of Materials 16 (11): 2187-2193.

SCHWARZENBACH, R. P.; GSCHWEND, P. M.; IMBODEN, D. M. (2003): *Environmental Organic Chemistry*. 2nd edition. Hoboken, New Jersey: John Wiley & Sons, Inc.

SHIN, M.-C.; CHOI, H.-D.; KIM, D.-H.; BAEK, K. (2008): *Effect of surfactant on reductive dechlorination of trichloroethylene by zero-valent iron.* Desalination 223: 299-307.

SWRCB (2014): *Groundwater information sheet: Tetrachloroethylene (PCE*). State Water Resources Control Board, Division of Water Quality, California Environmental Protection Agency. online: http://www.waterboards.ca.gov/gama/docs/coc_pce.pdf (08.06.2017)

VAN LIEDEKERKE, M.; PROKOP, G.; RABL-BERGER, S.; KIBBLEWHITE, M.; LOUWAGIE, G. (2014): *Progress in the Management of Contaminated Sites in Europe.* Luxembourg: Publications Office of the European Union. online: http://publications.jrc.ec.europa.eu/repository/bitstream/111111111/30755/1/lbna26376enn.pdf (08.06.2017)

VIPULANANDAN, C.; REN, X. (2000): *Enhanced Solubility and Biodegradation of Naphthalene with Biosurfactant.* Journal of Environmental Engineering 126 (7): 629-634.

VOLKERING, F.; BREURE, A. M.; VAN ANDEL, J. G.; RULKENS, W. H. (1995): *Influence of Nonionic Surfactants on Bioavailability and Biodegradation of Polycyclic Aromatic Hydrocarbons.* Applied and Environmental Microbiology 61 (5): 1699-1705.

WANG, C.B.; ZHANG, W.X. (1997): *Synthesizing nanoscale iron particles for rapid and complete dechlorination of TCE and PCBs*. Environmental Science & Technology 31: 2154-2156.

WEISGRAM, M.; BRANDNER, P.; FODITSCH, S.; DÖRRIE, T.; MÜLLER, D. (2012): *ARBEITSHILFE CKW - KONTAMINIERTE STANDORTE. Methoden der Erkundung, Beurteilung und Sanierung von CKW-kontaminierten Standorten.* Wien: Österreichischer Verein für Altlastenmanagement (ÖVA). online: http://www.blpgeo.at/download/ckw-kontaminierte-standorte (08.06.2017)

WOLLRAB, A. (2009): *Organische Chemie. Eine Einführung für Lehramts- und Nebenfachstudenten.* 3rd edition. Berlin, Heidelberg: Springer-Verlag

ZHANG, M.; HE, F.; ZHAO, D.; HAO, X. (2011): *Degradation of soil-sorbed trichloroethylene by stabilized zero valent iron nanoparticles: Effects of sorption, surfactants, and natural organic matter*. Water Research 45: 2401-2414.

ZHANG, Y.; MILLER, R. M. (1995): *Effect of Rhamnolipid (Biosurfactant) Structure on Solubilization and Biodegradation of n-Alkanes*. Applied and Environmental Microbiology 61 (6): 2247-2251.

ZHANG, W. (2003): *Nanoscale iron particles for environmental remediation: An overview.* Journal of Nanoparticle Research 5: 323-332.

ZHAO, G.; CHASTEEN, N. D. (2006): *Oxidation of Good's buffers by hydrogen peroxide.* Analytical Biochemistry 349: 262–267.

APPENDIX

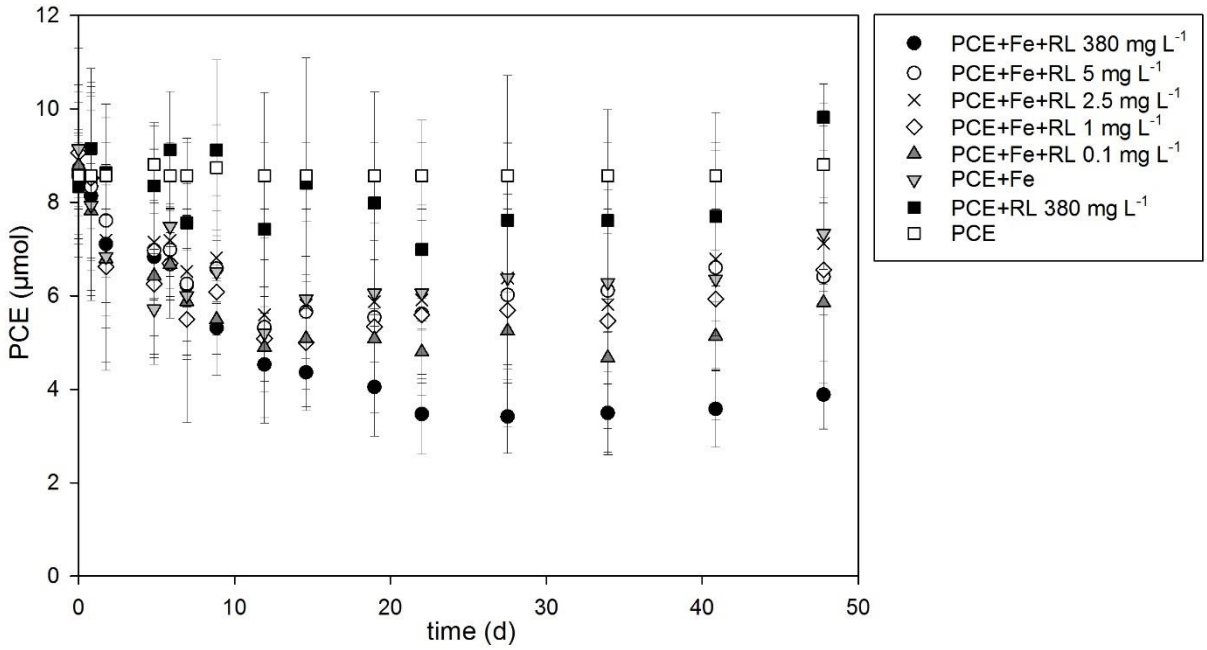

App. 1: Decrease in PCE (µmol) with values corrected for loss of PCE in all treatment groups over time of the experiment (*n=3*); control group with only PCE slightly deviating on day 5, 9 and 48 because *n=2*

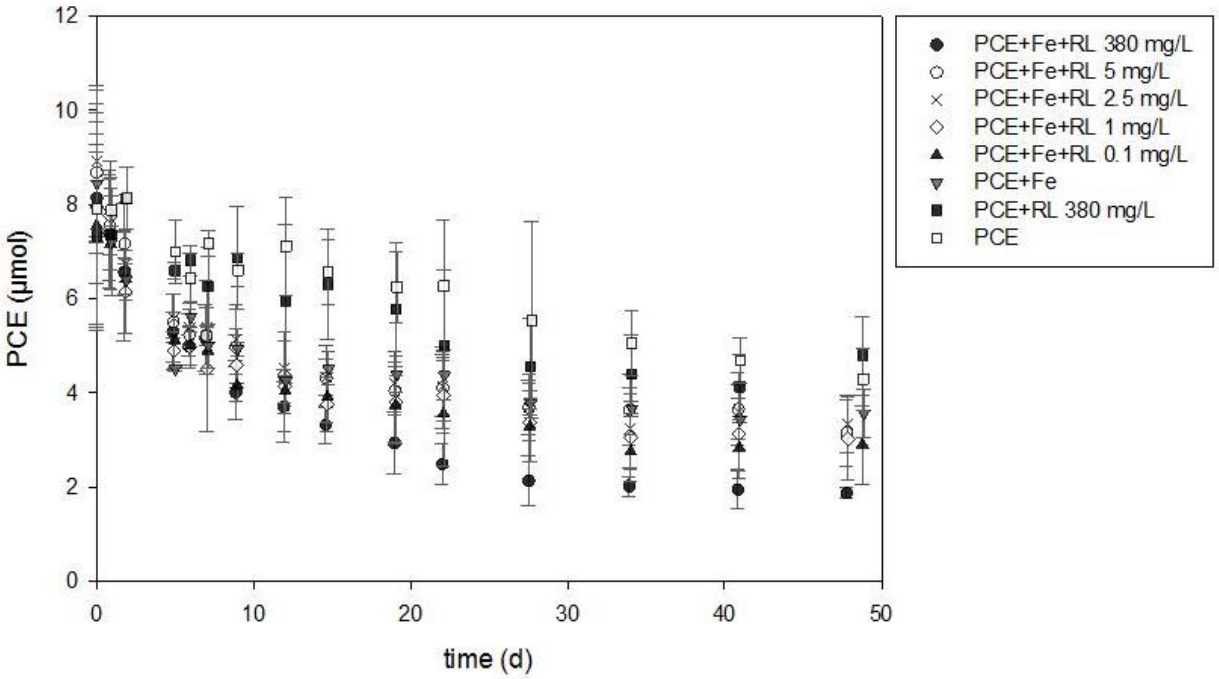

App. 2: Decrease in PCE (µmol) with values uncorrected for loss of PCE in all treatment groups over time of the experiment (*n=3*); control group with only PCE slightly deviating on day 5, 9 and 48 because *n=2*